

An observational study on the effect of L-ornithine-L- aspartate (LOLA) on the gut microbiome in liver cirrhosis. A monocentric, observational phase 4 study

Daniel Habich, Angela Horvath, Nicole Feldbacher, Lavra Rebol, Rosa Haller, Kristina Zukauskaitė,
Vanessa Stadlbauer

9.7.2025

Contents

Abstract	4
Background	4
Materials and Methods	4
Results.....	4
Conclusion	5
Introduction	6
Methods.....	8
Trial Design	8
Participants	8
Recruitment	8
Inclusion & Exclusion	8
Study conduct	8
Intervention	9
Sample size	9
Blood and Stool sampling, routine blood analysis	9
Microbiome analysis	10
Quality of life and sarcopenia measures.....	11
Sarcopenia, gut permeability, bacterial translocation biomarkers.....	11
Metabolomics analysis.....	11
Statistical methods	12
Metadata analysis.....	12
Microbiome analysis	13
Metabolomics Analysis	14
Results	14
Baseline characteristics	14
The abundance of the genus <i>Flavonifractor</i> remained unaffected by LOLA Treatment	16
Bacterial alpha and beta diversity were not affected by LOLA.....	16
Influence of LOLA on the microbial composition.....	17
Identification of microbiome features associated with the intervention/timepoint	19
LOLA was not associated with changes in predicted gut microbiome function	19
Perceived Vitality (Quality of live) improved by the treatment.....	20
Liver frailty index, SARC-F and index ALD was not affected by the LOLA intervention	21
Appendicular skeletal and lean muscle mass reduced during the intake of LOLA	22
Anthropometric muscle parameters were not influenced by the intervention	24
Influence of LOLA on routine biochemistry	24

Sarcopenia biomarkers were not affected by the intervention..... 26

LOLA intervention was associated with improvement of intestinal permeability and inflammatory response towards endotoxin 27

LOLA intervention was associated with changes in serum, stool and urine metabolites..... 28

Associations between biomarkers, gut health, and clinical factors..... 31

Safety and Adherence to LOLA 32

Subgroup analyses 35

 High versus low baseline ammonia 35

 Gender differences 35

Discussion 37

Conclusion 40

 Data availability 41

References 42

Abstract

Background

Liver cirrhosis is associated with gut microbiome dysbiosis, intestinal inflammation and gut barrier dysfunction, contributing to reduced quality of life and the development of complications. In a recent retrospective study, we showed that L-ornithine-L-aspartate (LOLA) was associated with improvement in taxonomic composition of the microbiome. We aimed to study prospectively, whether LOLA can improve gut microbiome dysbiosis and function, sarcopenia, frailty, ammonia levels and quality of life.

Materials and Methods

In a monocentric, open-label, phase 4 study, patients with liver cirrhosis and hepatic encephalopathy grade 0-2 (assessed by either number connection test or critical flicker frequency or Westhaven criteria) received LOLA 18g/day orally for 3 months. We studied gut microbiome composition and function (16S rRNA gene sequencing, analysis of alpha and beta diversity, taxonomic differences assessed by LEfSe and paired Wilcoxon rank sum test, Tax4fun to predict function), quality of life (short form 36 questionnaire, SF36), serum ammonia, measurements of sarcopenia and frailty (appendicular lean muscle mass, anthropometric measures, liver frailty index, SARC-F), biomarkers of sarcopenia (myostatin, irisin, fibroblast growth factor (FGF)-21, insulin like growth factor (IGF-1)), biomarkers for gut permeability and inflammation (soluble CD14 (sCD14), LPS binding protein (LBP), calprotectin, zonulin, diamine oxidase (DAO)) and alterations in the metabolome (Nuclear Magnetic Resonance (NMR) spectrometry in stool, serum and urine).

Results

258 patients were screened, 65 included and 52 patients (40.4% female, age 62 (58; 65)) completed the study. LOLA intake did not influence the abundance of *Flavonifractor* or *Oscillospira* in the gut microbiome. LOLA intake decreased the abundance of the genus *Romboutsia* but did not alter microbiome diversity or predicted function. LOLA significantly improved the SF36 dimension vitality (from 45 (35; 60) to 50 (45; 60), $p=0.019$). LOLA also decreased serum ammonia in patients with elevated baseline values ($n=10$; from 69.5 (54; 225) $\mu\text{mol/L}$ to 46.0 (22; 66) $\mu\text{mol/L}$, $p=0.004$). Muscle mass declined over the study period in many patients, but not in the subgroup of patients with elevated and subsequently improved ammonia levels. Sarcopenia, frailty scores, muscle biomarker and biomarker for gut inflammations and gut permeability (calprotectin, zonulin, sCD14) did not improve either. However, DAO, as a marker of gut barrier dysfunction, decreased significantly (from 12.75 U/mL (11.25; 17.45) to 11.15 U/mL (9.9; 15.65), $p=0.016$) and LBP, as a marker of innate immune response to bacterial translocation, increased significantly (from 17.05 $\mu\text{g/mg}$ (14.7; 19.8) to 17.39 $\mu\text{g/mg}$ (16.2;

21.9), $p=0.006$). Metabolomic analysis indicated significant intervention associated changes in alanine levels and slight changes in other amino acids and lipoproteins.

Conclusion

LOLA improved vitality in patients with cirrhosis, a clinically relevant patient reported outcome parameter. LOLA also improve intestinal permeability, innate immune response and altered microbiome composition as well as amino acid profiles in the whole cohort. LOLA prevented muscle loss only in patients with elevated ammonia levels at baseline. LOLA may therefore be a useful adjunct treatment to improve quality of life in cirrhosis and to prevent muscle loss in hyperammonemic patients.

Introduction

Chronic liver diseases and liver cirrhosis are on the rise in Europe, especially alcohol related cirrhosis (1,2). Cirrhosis is associated with a more than six-fold increase in-hospital mortality, mainly due to complications such as infections, renal failure, hepatic encephalopathy, bleeding, or sarcopenia (2). The gut microbiome is currently understood as a key driver of complications of cirrhosis (3). Gut microbiome composition has been found to be severely altered in liver cirrhosis in general with a reduction in bacterial diversity and an increase in potential pathogens (4). Factors influencing the microbiome in cirrhosis are etiology and severity of liver disease, drug intake, nutritional status and inflammation (5). Gut microbiome dysbiosis in cirrhosis is further associated with alterations in gut permeability, bacterial translocation and immune reaction, attributing to the risk of complications and mortality (6). In general, many human-targeted drugs can alter the composition of the gut microbiome (7). So far mainly negative effects of drugs on the gut microbiome have been described (7,8). Positive modulations of the gut microbiome may be achieved using pre- or probiotics (9–12). However, systematic assessments of already licensed drugs are lacking. One commonly used drug in liver cirrhosis is L-ornithine-L-aspartate (LOLA). The amino acids L-ornithine and L-aspartate in LOLA dissociate readily and are consecutively absorbed. L-ornithine serves as an intermediary in the urea cycle in periportal hepatocytes in the liver and as an activator of carbamoyl phosphate synthetase, and both amino acids also lower ammonia levels by transamination to glutamate via glutamine synthetase in perivenous hepatocytes as well as by skeletal muscle and brain (13). Therefore, it is used as an ammonia-lowering agent in patients with covert or overt hepatic encephalopathy. Hepatic encephalopathy (HE) is one of the most debilitating complications of cirrhosis and associated with increased morbidity and mortality (14). Although the pathogenesis is still incompletely understood, nowadays it is assumed that protein and urea breakdown by colonic bacteria leads to ammonia release and due to the reduced capacity of the liver to detoxify, ammonia accumulates and is shunted into the systemic circulation (15,16). Ammonia accumulates in the brain and has neurotoxic effects, especially on astrocytes (17,18). LOLA is therefore part of the standard regimen to treat hepatic encephalopathy and prevent further episodes. (19) Besides these direct effects on hepatic encephalopathy, also additional functions of LOLA, such as hepatoprotective effects or effects on restoring skeletal muscle proteostasis, have been proposed but are not fully explained to date (20). Since oral LOLA encounters the human gut microbiome and the intestinal barrier first, effects on the gut microbiome and intestinal permeability may play a role in the clinical effects of LOLA. We recently showed in a retrospective setting for long-term LOLA treatment, that in the microbiome, the genera *Flavonifractor* and *Oscillospira* were more abundant in patients treated with LOLA compared to the control group, while alpha and beta diversity were comparable between groups (21). Differences in stool and serum metabolomes reflected the pathophysiology of hepatic encephalopathy and confirmed LOLA intake. In

the urine metabolome, the ethanol to acetic acid ratio was lower in patients treated with LOLA compared to controls. Patients treated with LOLA also showed lower serum levels of insulin-like growth factor 1 (IGF-1) than patients without LOLA treatment. No differences in gut permeability or inflammation markers were found in our retrospective study. Higher abundance of *Flavonifractor* and *Oscillospira* in LOLA treated patients could indicate LOLA as a potential microbiome modulating strategy in patients with liver disease. The lower levels of IGF-1 in patients treated with LOLA suggest a possible link between the pathophysiology of hepatic encephalopathy and muscle health (21).

Here we conducted a monocentric, observational phase 4 study, to test the effects of a three-month long intervention with LOLA in cirrhotic patients, on the abundance of the genus *Flavonifractor*, a change in alpha or beta diversity, a shift in the taxonomic composition or predicted gut microbiome function. Further, stool serum or urine metabolome composition, ammonia blood levels as well as biomarkers of gut permeability were assessed. Sarcopenia was assessed via anthropometric measurements, hand grip strength, gait speed, balance or a change in muscle mass as well as assessment of the liver frailty index. Quality of life was assessed via short form (SF)-36, SARC-F and Barthel activities of daily living (ADL) index.

Methods

Trial Design

Monocentric open observational phase IV study in 65 patients with liver cirrhosis. The study protocol was approved by the institutional review board of the Medical University of Graz (35-028ex22/23) registered at ClinicalTrials.gov (NCT05737030).

Participants

Recruitment

Patients were recruited from 07.02.2023 to 29.04.2024 at the outpatient clinic at the Department of Gastroenterology and Hepatology at the Medical University of Graz by chart review for prescreening and inviting potentially eligible patients for screening by the staff hepatologists.

Inclusion & Exclusion

Adult patients (18 years of age or older) with the diagnosis of liver cirrhosis using clinical, imaging or histopathological tests and have hepatic encephalopathy (Grade 0-2) diagnosed either through Westhaven criteria (overt HE – HE grade 1-2) or a critical flicker frequency below 39 Hz and/or a number connection test A over 30 seconds (covert HE – HE grade 0) were eligible after signing a written informed consent and accepting the usage, publication and confidential use of their encoded data. Exclusion criteria included: allergies to LOLA or its constituents (or medication with similar chemical structure), recent changes in medication-dose of lactulose therapy for HE, intake of antibiotics, LOLA or L-dopamine, renal insufficiency or hepatocellular carcinoma, pregnancy or breastfeeding.

Study conduct

Study related procedures were performed by trained personnel according to ICH-GCP guidelines, visits were undertaken on an outpatient basis. The study was monitored by the Coordination Center for Clinical Studies from medical University of Graz. At baseline (T0) and at the end of the intervention (T1), detailed medical history (past and present diagnoses, concomitant medication, comorbidities, complications of liver cirrhosis and adverse events), demographic parameters (gender, age, date of birth), lifestyle factors (physical activity, smoking, alcohol consumption), type of diet (food preference questionnaire) as well as vital signs (blood pressure, heart rate) were collected. Anthropometric data (weight, height, mid-arm muscle circumference, triceps skinfold thickness), handgrip strength (HGS), balance and gait speed and body composition using dual X-ray absorptiometry (DXA) were collected and measured and liver frailty index was calculated. Blood, serum, urine and stool samples were collected for analysis of research biomarkers. Liver disease severity scores were calculated from

laboratory and clinical data (Child-Pugh and MELD). Quality of life was assessed using the SF-36, SARC-F and Barthel ADL index, before the three-month long intervention with LOLA. Collection of the patient data was performed using RedCap (Vanderbilt University, Nashville, USA).

An increase in abundance in the genus *Flavonifractor* after the three-month intervention period was considered as the pre-determined primary endpoint of the study. Several secondary outcome measures were defined, such as a change in quality of life, a change in alpha or beta diversity of the gut microbiome, a change in the taxonomic composition of the gut microbiome or a change in the predicted gut microbiome function after three months of LOLA treatment. Also, a change in quality of life, in muscle mass, handgrip strength, gait speed, anthropometric parameters; in blood ammonia levels and changes in biomarkers for gut permeability and inflammation; changes in the metabolic composition of stool, serum and urine, the occurrence of cirrhosis-complications as well as safety of the intervention were considered as secondary endpoints.

Biomarkers for sarcopenia gut inflammation and gut barrier function were assessed by ELISA. Microbiome composition was assessed by *16S rRNA* gene analysis from stool samples and metabolome composition was assessed by NMR spectrometry in stool, serum and urine samples. Detailed descriptions of the outcome assessment are given below.

Intervention

Hepa-Merz® Granulat 3g (Merz Therapeutics GmbH, Frankfurt, Germany), containing L-ornithine-L-aspartate as an orange-coloured granulate was administered as two sachets 3 times a day (18g in total), and consumed dissolved in a glass (200 ml) of water, tea or juice.

Sample size

In preliminary data, LOLA-users showed a relative *Flavonifractor* abundance of 0.0041 as compared to non-users of 0.00071. Standard deviation was 0.0058. To detect a difference like this before and after a 3-months LOLA-treatment with an alpha of 5% and a beta of 20%, 55 patients need to be included in the study (assuming a 20% dropout rate).

Blood and Stool sampling, routine blood analysis

For routine parameters, blood was sampled in EDTA, lithium-heparin and sodium-citrate tubes. For analysis of research parameters, blood was sampled in serum-, EDTA, sodium-citrate and lithium-heparin tubes. To get plasma, blood was centrifuged at 2000xg for 10 min; to get serum, blood samples were kept at room temperature for 30 minutes and then centrifuged. After centrifugation, plasma or serum was aliquoted under pyrogen-free conditions and stored at -80°C. Analysed routine blood

biochemistry parameters included: full blood count, electrolytes, renal function, liver function including ammonia, blood clotting and inflammation parameters. Reference values (median or ranges) for these values were applied according to the Clinical Institute for Medical and Chemical Laboratory Analysis at the University Hospital Graz. Liver disease severity scores were calculated from laboratory and clinical data (Child-Pugh and MELD). Stool samples were collected by the patients at home prior to the study visits in sterile collection tubes. Samples were aliquoted and frozen at -80°C upon arrival until further analysis.

Microbiome analysis

For microbiome analysis, stool samples were thawed, and DNA was isolated using the SphaeraMag® Genomic DNA Fecal Purification Kit (Procomcure Biotech). Samples have been processed individually in tubes to minimize the risk of cross-contamination. Library preparations and sequencing were done according to the Illumina protocol. Hypervariable regions V1-V2 were amplified using the primers 27F-AGAGTTTGATCCTGGCTCAG; R357-CTGCTGCCTYCCGTA. Sequencing was done with an Illumina NextSeq2000 instrument according to the application note. The quality of the raw sequencing data was checked with FastQC and MultiQC implemented in a local Galaxy instance. Based on the quality report, truncating parameters were set to 250 and 250 for forward and reverse reads, respectively. Furthermore, the first 10 bases of all reads were trimmed given the non-random distribution of bases in this area. Trimmed and truncated reads were handed off to the dada2 inference algorithm made available through QIIME2 (22) tools. Denoising was performed independently with a maximum error rate of 2 for both forward and reverse reads. Reads were truncated at the first instance of a quality score less than 2, and the minimum merging region was defined as 12 bases. Chimera detection was performed in consensus mode, with the minimum abundance of potential parents of a sequence being tested as chimeric being set to 1. The error model was trained on 1.000.000 random reads. A naïve Bayesian classifier was trained on the SILVA database version 138 with a release threshold of 99% identity. A phylogenetic tree was built by creating a sequence alignment using MAFFT, after which any alignment columns that are phylogenetically uninformative or ambiguously aligned were removed. The resulting masked alignment was used to infer a phylogenetic tree and then subsequently root it at its midpoint using FastTree. The resulting count table, classification, and rooted tree were then exported as .qza files for import into the R-based CBmed Microbiome Analysis Platform for further data cleaning and statistical analysis as described below. Raw sequence data are deposited in the National Center for Biotechnology Information sequence read archive (NCBI SRA, accession no. PRJNA1223152).

Quality of life and sarcopenia measures

Quality of life was assessed via the SF-36 questionnaire (23) and neuromuscular or musculoskeletal disorders were measured with the Barthel ADL Index (24). Reference values for SF-36 scores were applied according to (25). Suggestive signs of sarcopenia were screened with the SARC-F questionnaire (26). Hand grip strength (HGS) (27), gait speed (timed 4-m walk) (28), balance (29), triceps skinfold thickness (TSFT) and mid-arm muscle circumference (MAMC) (30) were assessed as previously described. BMD via DXA was performed using the Lunar iDXA system (GE Healthcare GmbH, Vienna, Austria) at the Department of Endocrinology, Medical University of Graz (31). Appendicular skeletal muscle mass (ASM), appendicular skeletal muscle mass index (ASMI) and appendicular lean muscle mass (ALM) were calculated as the EWGSOP2 recommended (32). Reference values for ASM, ASMI and ALM were applied according to (33,34). Liver frailty index (LFI) was calculated according to (35) using the measured parameters of average (3 attempts) dominant hand grip strength (HGS), time for 5 chair raises (chair raise per sec) and the total time of balancing capabilities for side, semi-tandem and tandem. Gender adjusted HSG was calculated as follows: for males average HSG was subtracted with 34.175 and then divided by 9.976; for females average HSG was subtracted with 21.863 and then divided by 6.312 (personal communication with (35)). Reference values for LFI were applied according to (35).

Sarcopenia, gut permeability, bacterial translocation biomarkers

Biomarkers for sarcopenia, gut permeability, bacterial translocation, and innate immune response were assessed by ELISA. ELIA kits for Diamine oxidase (DAO, serum), zonulin (stool), calprotectin (stool), myostatin (EDTA plasma) were purchased from Immundiagnostik, Bensheim, Germany); ELISA kits for Insulin-like growth factor-1 (IGF-1 EDTA), FGF21 (EDTA plasma) and sCD14 from Bio-Techne, Minneapolis, MN, USA; ELISA kits for irisin (EDTA) from Biovendor, Brno, Czech Republic; and ELISA kits for lipopolysaccharide binding protein (LBP, EDTA plasma) from Hycult Biotech, Uden, The Netherlands). All assays were performed according to the manufacturer's instructions without modifications, with reference values applied as specified in the results section.

Metabolomics analysis

Lipoproteins, small molecular metabolites, and glycoproteins of serum samples were measured on a Bruker 600 MHz Avance Neo NMR spectrometer (Bruker, Rheinstetten, Germany) as described previously (36). Serum samples were thawed, and 300 μ L of each sample were mixed with 300 μ L of Bruker serum buffer (Bruker, Rheinstetten, Germany). For urine analysis, 540 μ L of each sample were mixed with 60 μ L of Bruker urine buffer. Samples were measured in 5 mm glass tubes and placed into a SampleJet rack (Bruker, Rheinstetten, Germany). Proton spectra were obtained at a constant temperature of 310 K using a standard nuclear Overhauser effect spectroscopy (NOESY) pulse sequence (Bruker: noesygppr1d), a Carr–Purcell–Meiboom–Gill (CPMG) pulse sequence with pre-

saturation during the relaxation delay (Bruker: cpmgpr1d) to achieve water suppression, a fast scan 2D J-resolved (JRES) pulse sequence (Bruker: jresgpprpf), and J-edited diffusional ¹H-NMR spectra (JEDI or PGPE, respectively) were recorded. Raw data analysis was carried out using the Bruker IVDr Plasma (B.I.) module (for the quantification of lipoproteins and small molecular metabolites), and the PhenoRisk PACS™ RuO module was used for quantifying glycoproteins in the analysis software (Topspin version 4.4, Bruker). Fecal samples for NMR spectroscopy measurements were prepared as previously described (36). Briefly, 200 μL of samples (50 to 100 mg of stool in 2 mL of DNA/RNA shield) were mixed with 400 μL methanol to inactivate and precipitate proteins. The remaining solids were lysed using a Precellys homogenizer (Bertin Technologies SAS, Montigny-le-Bretonneux, France) and stored at -20 °C for 1 h, followed by centrifugation for 30 min at 10,000× g at 4 °C. Finally, the supernatants were lyophilized, resuspended in 500 μL NMR buffer (0.08 M Na₂HPO₄, 5 mM 3-(trimethylsilyl) propionic acid-2,2,3,3-d₄ sodium salt (TSP), and 0.04 (w/v) % NaN₃ in D₂O, with the pH adjusted to 7.4 with HCl or NaOH, respectively), and transferred into 5 mm NMR tubes for measurement on the NMR instrument using the CPMG pulse sequence as described. Spectra pre-processing and data analysis were carried out using MatlabR scripts (courtesy of Prof. Jeremy Nicholson, Imperial College London, London, UK). NMR data were imported to MatlabR vR2014b (Mathworks, Natick, MA, USA), with the regions around the water, TSP, and remaining methanol signals excluded, aligned, and corrected for the sample metabolite dilution by probabilistic quotient normalization. The reported values correspond to an arbitrary unit (A.U.) derived from the area under the peak being proportional to concentration.

Data preprocessing was performed using R (37). Only patients with samples from both timepoints were included in the analysis. Metabolites were filtered based on detection frequency: serum and stool metabolites had to appear in ≥80% of samples, and urine metabolites in ≥20%. Missing values, assumed to be below the limit of quantification, were imputed using quantile regression imputation for left-censored data (QRILC) (38) via the `impute.QRILC()` function from the `imputeLCMD` package (39).

Statistical methods

Metadata analysis

Clinical data (patient data, measured laboratory parameters, blood chemistry, etc.) were documented in paper based case report forms and in the patient charts as source data, transferred to RedCap and then exported from RedCap as .csv files, and imported into R-studio using the `read.csv` function from the `utils` package (40). Median and 95% confidence intervals of baseline characteristics were calculated using the `MedianCI` function from the `DescTools` package (41). For longitudinal data, differences between timepoints (delta values) were calculated and were tested for normality using the

shapiro.test function from the stats package (40). To test if longitudinal data changed over the course of the intervention, paired-t tests were conducted using the t.test function from the stats package (40) for data following normal distribution; for not normally distributed data, Wilcoxon rank sum tests were performed using the wilcox.test function from the stats package (40). Multiplicity control was performed with the p.adjust function from the stats package (40), using the Benjamin Hochberg correction. Significant changes from T0 to T1 were visualized as boxplots using the ggplot2 package (42).

Microbiome analysis

QIIME2 artifacts (.qza) of the count table, classification-file and the rooted tree together with a corresponding metadata file were imported into R-studio using the qza_to_phyloseq function from the qiime2R package (43). Contaminating sequences were removed using the isContaminant function from the decontam package (44). Mitochondrial and chloroplast ASVs were removed using the subset_taxa function from the package phyloseq (45). Taxa with an abundance of zero were removed using the prune_taxa function of the phyloseq package (45). After pre-processing, a median of 85402 (95% CI: 74963-92148) reads per sample was available: (range from 34501 to 299143). Visualizations of taxonomic composition were plotted using the packages mia (46) and ggplot2 (42). To calculate alpha diversity measures samples were rarefied to minimal sample size (sampling depth: 34501 reads) using the rarefy_even_depth function from the phyloseq package (45), before Faiths phylogenetic diversity was calculated using the function estimate_pf from the btools package (47) and species richness, Shannon diversity and inverted Simpson index were calculated using phyloseqs estimate_richness function (45). Evenness was calculated by dividing the Shannon diversity by the natural logarithm of the species richness. To check for differences in the alpha diversity measures from T0 to T1, a Wilcoxon ranked sum test was performed. For beta diversity the distance function from phyloseq (45) was used to calculate sample distance according to different distance metrics (Unifrac, weighted Unifrac, Bray-Curtis dissimilarity and Jaccard index); the ordinate function was used to create principal coordinates analysis (PCoA) which was plotted using phyloseqs plot_ordination function (45). Subsequent permutational multivariate analysis of variance (PERMANOVA) was performed using the adonis2 function from the vegan package (48). Redundancy analysis was performed with the rda function from the vegan package (48) and appendant analysis of variance (ANOVA) was conducted with the anova function from the stats package (40). To identify differentially abundant taxa between the groups and differences in the structural composition of the microbiome from T0 to T1 different tools were used. To determine features which most likely explain the difference between the two timepoints a linear discriminant analysis of the effect size (LEfSe) was conducted using the run_lefse function from the microbiomeMarker package (49). To identify features that are differential abundant between the two timepoints while accounting for compositional nature of the data an analysis of compositions of

microbiomes (ANCOM) was performed using the `run_ancom` function from the `microbiomeMarker` package (49). To identify linear associations between the timepoint and individual features, multivariate association analysis (MaAsLin2) was performed using the `Maaslin2` function from the `Maaslin2` package (50). To calculate differential abundance of the bacterial biomarkers *Oscillospira* and *Flavonifractor*, a taxonomy table was extracted from the `phyloseq` object via the `tax_table` function. All OTUs of these two genera were selected and combined to make a genus wide comparison of their abundance. To check their differential abundance a `wilcox.test` from the `stats` package (40) was performed. To assess predicted gut microbiome function, the tool `Tax4Fun`, implemented in the `MicrobiomeAnalyst` (51) platform, was used to generate a KEGG Orthology (KO) table. This was used for Functional Diversity Profiling (51), linking the predicted functions to specific metabolic systems.

Metabolomics Analysis

To assess whether the overall metabolome showed significant shifts throughout the study, a Permutational Multivariate Analysis of Variance (PERMANOVA) was performed using the `adonis2` function from the `vegan` package (48) after calculation of the Bray Curtis distance. To get an overview of the overall observable group separation between timepoints a Principal Component Analysis (PCA) was performed using `prcomp()` from the `stats` package for exploratory purposes and visualized with `ggplot2` (42). Datasets were \log_2 -transformed after QRILC imputation (38). PLS-DA was performed using the `mixOmics` package (52) to identify metabolites driving separation between T0 and T1. To account for inter-patient variability, a multilevel correction for paired data was applied using the `withinVariation()` function (52). Both \log_2 transformation and z-score scaling were performed on the data after imputation to standardize the metabolites. PLS-DA models were validated through cross-validation, with performance assessment using permutation-based significance testing via the `perf()` function (52). PLS-DA component plots were created to visualize timepoint separation, and Variable Importance in Projection (VIP) scores were calculated to assess the influence of each metabolite in distinguishing between groups. All plots were generated using `ggplot2` (42). Metabolite Set Enrichment Analysis (MSEA), using the KEGG pathway database as a reference, to identify enriched metabolic pathways associated with changes in metabolite concentrations (serum, stool, urine) between T0 and T1. Following imputation, datasets were normalized (TSS), \log_2 -transformed, and z-score scaled. Pre-processed data was uploaded to `MetaboAnalyst` (53) to perform MSEA.

Results

Baseline characteristics

From 258 patients who were screened for eligibility, 65 started the intervention with LOLA. 193 were not included because they did not meet inclusion criteria (n=30), met at least one of the exclusion

criteria (n=28) or declined to participate in the study (n=135). During the three-month intervention period, 14 patients (21.5%) dropped out of the study because of non-adherence to the study protocol (n=6), side effects from the product (n=3), lost to follow up (n=1), adverse events (n=1) and withdrawal of consent (n=1). In total, 52 patients finished the study per protocol and were included in the analysis. Figure 1 shows a flow diagram summarizing the enrolment of participants throughout the study.

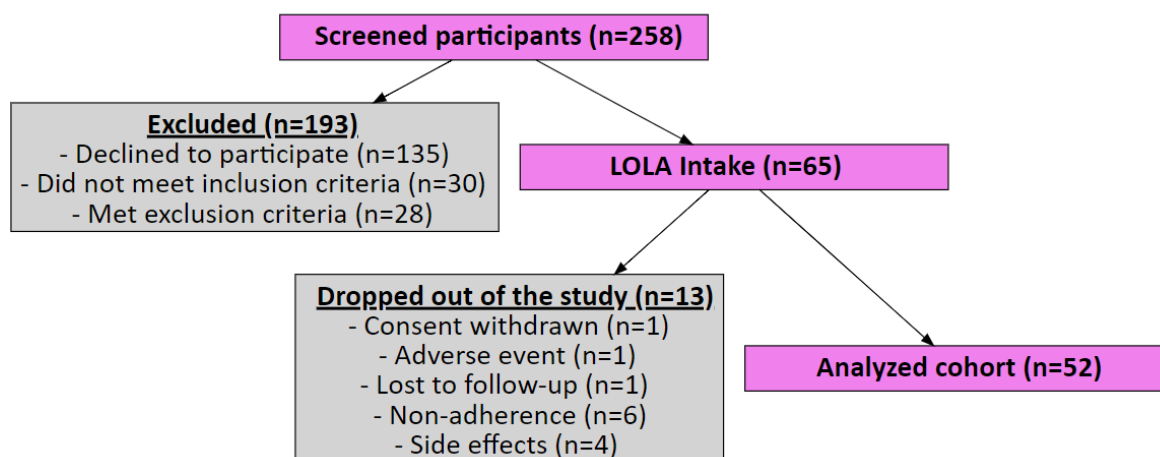


Figure 1: Patient flow chart

From 52 included patients, 40.4% (n=21) were female and 59.6% (n=31) were male, and the age ranged from 40 to 76 years with a median of 62 years (95% CI: 58-65). Patient characteristics are shown in Table 1.

Table 1: Baseline characteristics.

Characteristics	Female (n=21, 40.4%)	Male (n=31, 59.6%)	Total (n=52 / 100%)	Difference (m/f) [p-value]
Age (years)	64 (57;69)	60 (54;67)	62 (58/65)	0.412
BMI (kg/m ²)	25.2 (22.8;32.3)	27.6 (24.4;29.7)	26.6 (24.4;29)	0.478
Physical exercise (h/week)	4 (2;6)	0 (0;5)	3 (0;4)	0.572
Smoking (y/ex)	(7/6) / 46.7%	(8/7) / 53.3%	(15/13) / 100%	0.398
Packyears	15 (7;22.5)	18.8 (7.5;40)	16.9 (10;22.5)	0.489
Alcohol use (y/n)	1/20 (4.8%/95.2%)	7/24 (22.6%/77.4%)	8/44 (15.4%/84.6%)	0.013*
Alcohol use (days/week)	7	2 (1;7)	3 (1;7)	0.467
Alcohol use (g/week)	63	72 (18;378)	67.5 (18;378)	0.05*
Alcohol use (g/sitting)	9	36 (18;54)	27 (9;54)	0.025*
Diabetes	8 / 53.4%	7 / 46.6%	15 / 100%	-
Cholesterol lowering medication*	4 / 50%	4 / 50%	8 / 100%	-

Data is given as median value (95% CI) or number/percentage; * 7 patients took statins, one patient took ezetimibe

The abundance of the genus *Flavonifractor* remained unaffected by LOLA Treatment

Investigation of the relative abundance for the genera *Flavonifractor* (primary endpoint) and *Oscillospira* revealed that there was no significant change from T0 to T1 for both genera within the whole cohort (Figures 2 A-B). The genus *Flavonifractor* occurred in 48 of the 52 patients, where it was detected in 44 patients at T0 and in 47 patients at T1. Overall relative abundance of the genus *Flavonifractor* decreased (Figure 2A) but did not reach statistical significance ($p=0.343$). The genus *Oscillospira* occurred in 20 patients in total. The genus was detected in 16 patients at baseline and in 13 patients at T1. Its relative abundance increased (Figure 2B), however it did not reach statistical significance ($p=0.422$).

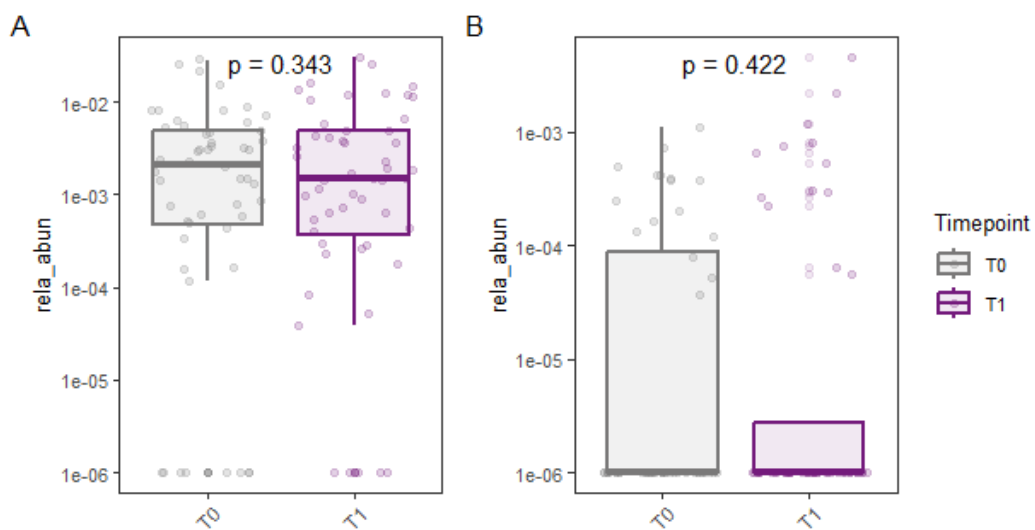


Figure 2: Relative abundance the bacterial genera *Flavonifractor* and *Oscillospira* at T0 and T1 (A) and (B) show results for the whole cohort ($n = 52$) were *Flavonifractor* occurs in 48 patients (T0: $n=44$; T1: $n=47$) and *Oscillospira* occurs in 20 patients (T0: $n=16$; T1: $n=13$). T0: baseline; T1: end of the intervention

Bacterial alpha and beta diversity were not affected by LOLA

LOLA intervention did not change alpha diversity (Figure 3) as measured by Species Richness ($p=0.948$), Shannon diversity index ($p=0.997$), inverted Simpson index ($p=0.946$), Evenness ($p=0.894$) and Phylogenetic diversity ($p=0.777$).

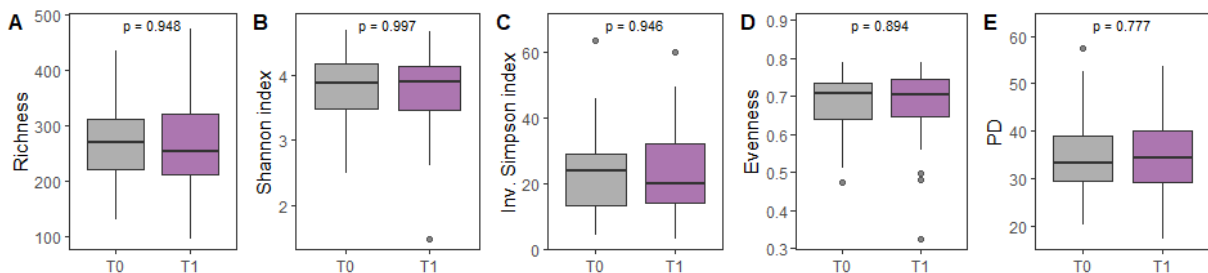


Figure 3: Alpha diversity indices at T0 and T1 for the whole cohort. (A) Species Richness; (B) Shannon diversity index; (C) inverted Simpson Index; (D) Evenness; (E) Phylogenetic diversity.

When investigating the impact of the intervention on different beta diversity measures, no significant differences could be detected within the whole cohort. Figure 4 displays 4 PCoA plots based on different distance metrics (Unifrac, weighted Unifrac, Bray-Curtis dissimilarities and Jaccard index) used to determine beta diversity.

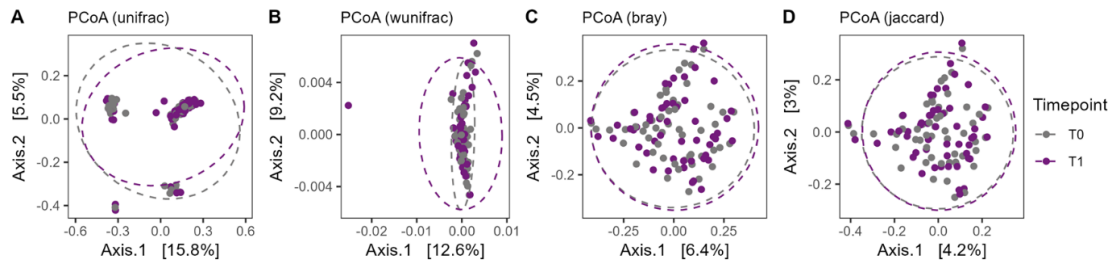


Figure 4: Beta diversity plots based on different distance methods; principal coordinate analysis was used for ordination. (A) Unifrac ($p = 0.84$); (B) weighted-Unifrac ($p = 0.97$); (C) Bray-Curtis Dissimilarity ($p = 1.00$); (D) Jaccard distance ($p = 1.00$).

Influence of LOLA on the microbial composition

Although individual taxa show a variation in abundance within individual patients from T0 to T1, for the whole cohort no major difference in the taxonomic composition (on phylum, class, order, family and genus level) was detected. The overall composition of the microbiome on different taxonomic levels at the two timepoints is shown in Figures 5A-E.

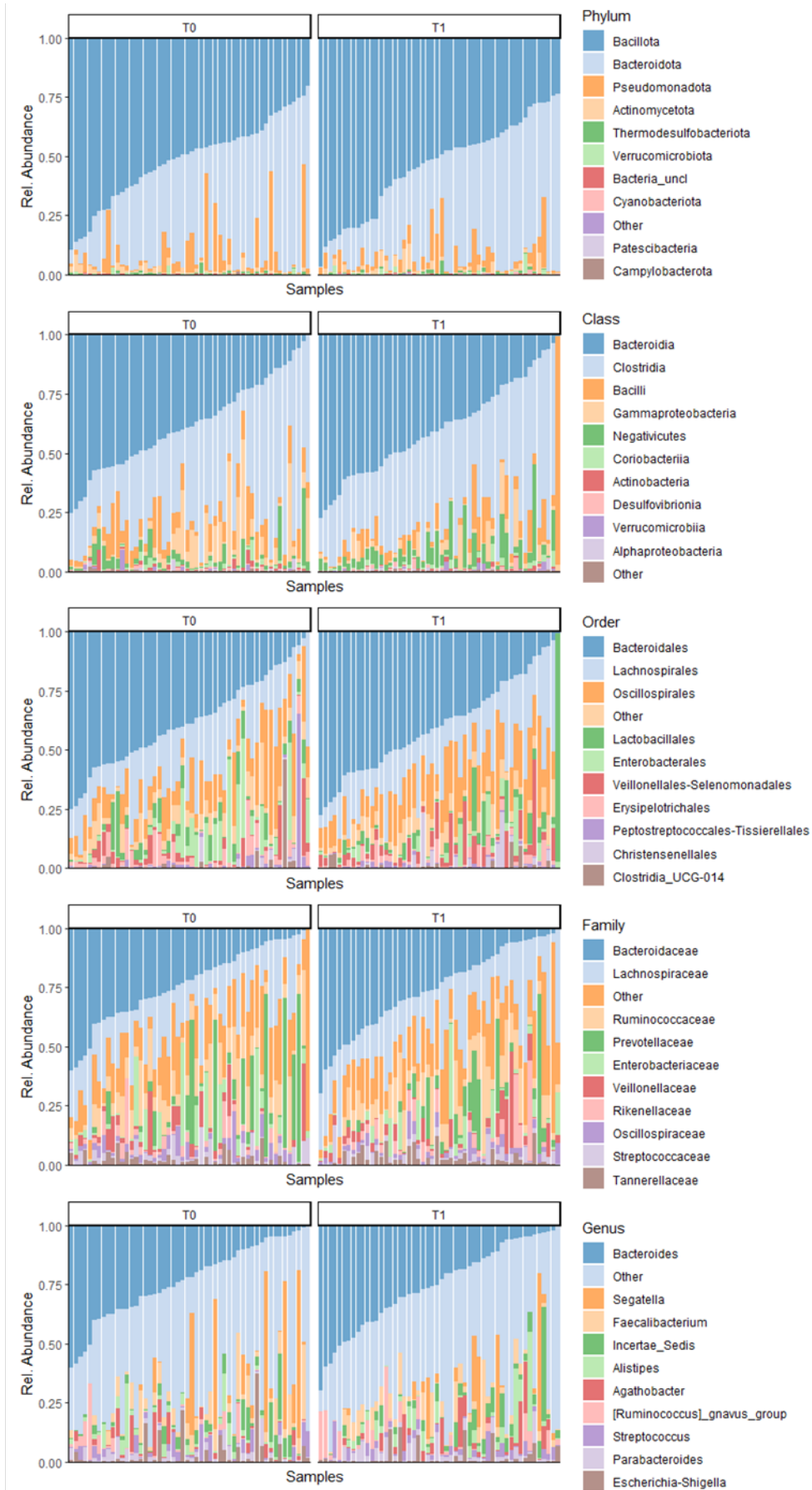


Figure 5: Taxonomic composition as relative abundance of all individual patients that participated in the intervention with LOLA; on Phylum, Class, Order, Family and Genus level, T0: baseline; T1: end of the intervention

Identification of microbiome features associated with the intervention/timepoint

LEfSe analysis was used to investigate potential bacterial biomarkers that are associated with one of the timepoints within the whole cohort, to show potential effects of LOLA on the modulation of the bacterial gut communities. With an LDA cutoff of 4, three features were identified to be enriched in one of the timepoints (the genus *Romboutsia* in T0 ($p < 0.001$); the family *Enterococcaceae* and the genus *Enterococcus* in T1 ($p = 0.03$); Figure 6A). Since LEfSe analysis is not validated for paired samples, a paired Wilcoxon Rank Sum test was performed to validate these results. For *Romboutsia* the median relative abundance dropped from 0.04 % (95% CI: 0.024 - 0.15) to 0.0034 % (95% CI: 0.0 - 0.025, $p < 0.001$; Figure 6B). For *Enterococcaceae* family and the *Enterococcus* genus identified, the median relative abundance increased from 0.0001% (95%CI: 0.0001-0.004) to 0.007% (95%CI: 0.0001-0.03; $p = 0.042$) (Figures 6C-D).

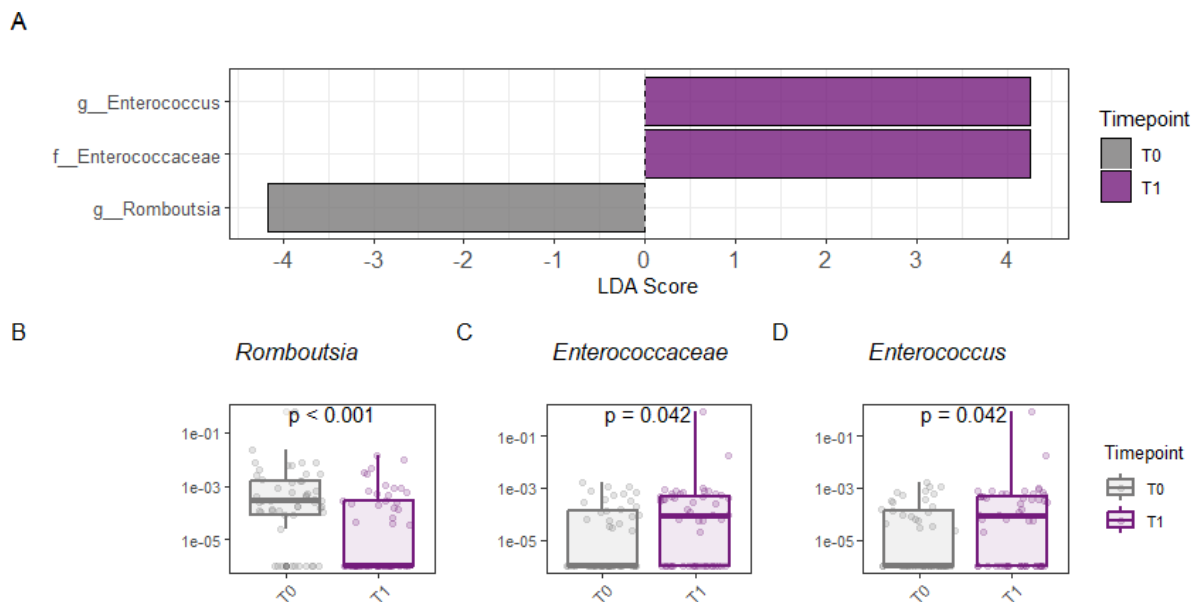


Figure 6: Results of Linear discriminant analysis Effect Size (LEfSe) analysis. (A) Linear discriminant analysis (LDA) plot of enriched taxa for each timepoint (LDA cutoff = 4); (B-D) Distribution of relative abundance for taxa identified through LEfSe at T0 and T1. T0: baseline; T1: end of the intervention.

LOLA was not associated with changes in predicted gut microbiome function

To evaluate changes in the functional potential of microbial communities during the intervention, we used Tax4Fun, implemented via the MicrobiomeAnalyst platform (51), to generate a KO table. This table contained 2,925 predicted functions associated with the microbial communities of the 52 patients included in the study. The KO table was subsequently utilized for Functional Diversity Profiling on Microbiome Analyst (51), linking the predicted functions to specific metabolic systems. However, no significant changes within the cohort were observed from T0 to T1 (Figure 7).



Figure 7: Predicted functional taxonomy as relative abundance of all individual patients that participated in the intervention with LOLA. Individual predicted functions were assigned to amino acid metabolism, biosynthesis of secondary metabolites, carbohydrate metabolism, energy metabolism, glycan biosynthesis and metabolism, lipid metabolism, metabolism of cofactors and vitamins, other amino acids, terpenoids and polyketides, nucleotide metabolism, and xenobiotic biodegradation and metabolism. T0: baseline; T1: end of the intervention

Perceived Vitality (Quality of live) improved by the treatment

All SF-36 items were significantly lower at T0 compared to the general population (Table 2). SF36-Vitality score (contains questions related to energy and fatigue) significantly improved during the intervention from 45 (95% CI: 35; 60) to 50 (95% CI: 45-60; p = 0.019; Figure 8A). The remaining SF36 items (physical functioning, bodily pain, general health perceptions, physical role functioning, emotional role functioning, social role functioning, mental health) remained unchanged by the intervention.

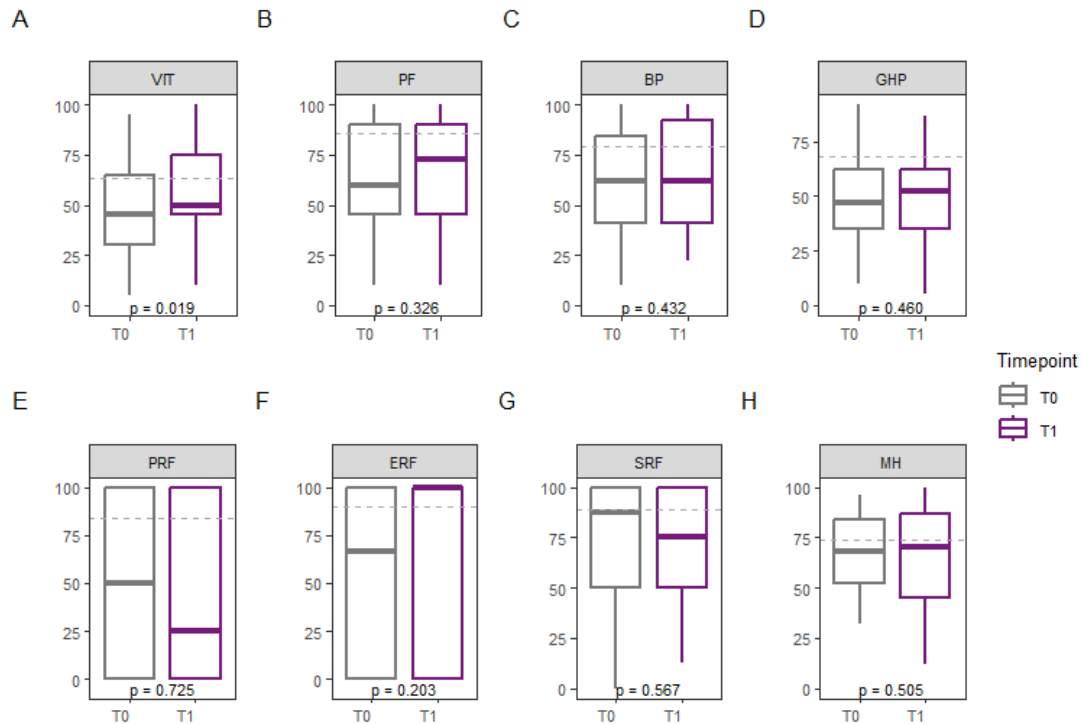


Figure 8: SF-36 items at T0 and T1: (A) Vitality ($p_{adj} = 0.155$), (B) Physical functioning ($p_{adj} = 0.648$), (C) bodily pain ($p_{adj} = 0.648$), (D) general health perception ($p_{adj} = 0.648$), (E) Physical role functioning ($p_{adj} = 0.725$), (F) emotional role functioning ($p_{adj} = 0.648$), (G) social role functioning ($p_{adj} = 0.648$), (H) mental health ($p_{adj} = 0.648$). The dashed line represents the median of a normal cohort according to (25). T0: baseline; T1: end of the intervention

Table 2: Mean scores of SF36 items, mean values and standard deviations from a random sample of the general German population according to (25), compared by Welch test.

	T0		Normal Cohort		t.test
	Mean	SD	Mean	SD	p value
Vit	46.3	22.91	63.27	18.55	<0.001
PF	63.62	25.23	87.71	24.49	<0.001
BP	61.86	29.25	79.08	27.87	<0.001
GHP	48.49	21.07	68.05	19.66	<0.001
PRF	49.44	43.46	83.7	37.28	<0.001
ERF	55.8	43.92	90.35	30.63	<0.001
SRF	72.45	28.18	88.76	19.98	<0.001
MH	65.04	21	73.88	17.53	0.003

T0: baseline

Liver frailty index, SARC-F and index ALD was not affected by the LOLA intervention

Liver frailty index remained unchanged from T0 to T1. At T0 the median value was 3.87 (95% CI: 3.63-4.15) and at T1 the value was 3.81 (95% CI: 3.54-4.12; $p=0.974$; Figure 9A). SARC-F scores for the whole cohort showed no significant changes from T0 to T1 (median value T0: 2 (95% CI: 1-2); T1: 1 (95% CI: 0-2; $p=0.98$; Figure 9B)). Patients whose SARC-F score at T0 was higher than 4 ($n = 7$) were investigated as individual subgroup, however there was also no significant change in the median SARC-F score for these patients (median value at T0: 5 (95% CI: 4-7); median value at T1: 4 (95% CI: 1-6; $p=0.151$; Figure 9C). The Barthel ADL index did not change significantly throughout the intervention. The median value

at T0 was 100 points (95% CI: 100 – 100) and remained unaltered at T1 at 100 points (95% CI: 95 – 100, $p=0.302$, Figure 9D), since most patients did not report any limitations in their activities of daily living.

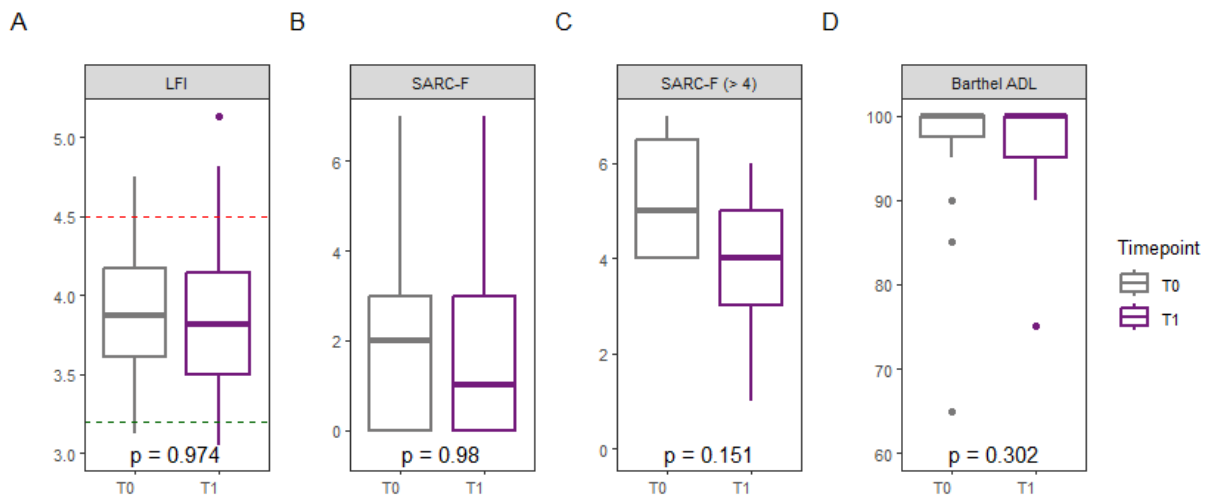


Figure 9: Different clinical indices: (A) Liver frailty index at T0 and T1. Dashed lines represent the reference range according to (35); (B) Muscle SARC-F score for the whole cohort; (C) Muscle SARC-F score for patients with a higher median SARC-F score than 4 at T0 ($n = 7$); (D) Barthel ADL index; from baseline (T0) to the end of intervention (T1).

Appendicular skeletal and lean muscle mass reduced during the intake of LOLA

After the three-month long intervention with LOLA, values for ASM, AMMI and ALM significantly decreased compared to T0. Median values decreased for ASM from 21.73 kg (95% CI: 19612-24174) to 19.99 kg (95% CI: 18456-23704; $p=0.002$; Figure 10A), for ASMI from 7.39 kg/m² (95% CI: 7.00-7.99) to 7.145 kg/m² (95% CI: 6.47-7.95; $p=0.023$; Figure 10B) and for ALM from 23.33 kg (95% CI: 20718-25766) to 22.46 kg (95% CI: 19764-25550; $p=0.013$; Figure 10C). However, within the subgroup of patients ($n=10$) with elevated ammonia levels at T0 (above 50 $\mu\text{mol/L}$), the values for ASM, AMMI and ALM remained unchanged throughout the intervention. (Figure 10D-F, Table 3)

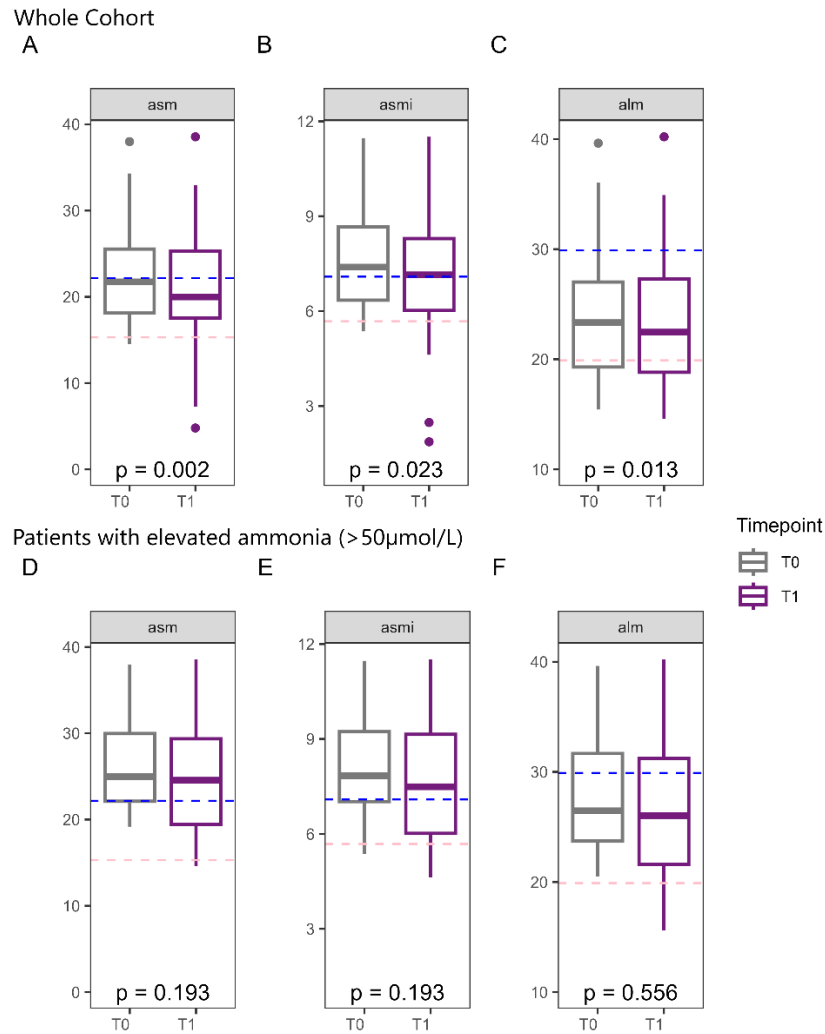


Figure 10: Muscle parameters at T0 and T1; A-C whole cohort: (A) appendicular skeletal muscle mass [kg]; (B) appendicular skeletal muscle mass index [kg/m²]; (C) appendicular lean muscle mass [kg]; D-F patients with elevated ammonia (>50µmol/L): (D) appendicular skeletal muscle mass [kg]; (E) appendicular skeletal muscle mass index [kg/m²]; (F) appendicular lean muscle mass [kg] Dashed lines represent the reference median values (blue = males, pink = females) according to (33,34). T0: baseline; T1: end of the intervention

Table 3: Level of appendicular muscle mass at T0 and T1, for whole cohort and subgroup with elevated ammonia at T0.

Parameter	Unit	T0	95% CI	T1	95% CI	p-value
ASM (whole cohort)	kg	21.73	19.61-24.17	19.99	18.45-23.70	0.002*
ASMI (whole cohort)	kg/m ²	7.39	7.00-7.99	7.145	6.47-7.95	0.023*
ALM (whole cohort)	kg	23.32	20.71-25.76	22.46	19.76-25.55	0.013*
ALMI (whole cohort)	kg/m ²	7.84	7.45-8.41	7.86	7.16-8.40	0.107
ASM (NH ₃ >50µmol/L)	kg	24.98	20.24-30.16	24.55	17.91-31.35	0.193
ASMI (NH ₃ >50µmol/L)	kg/m ²	7.84	7.00-9.63	7.49	5.46-10.01	0.193
ALM (NH ₃ >50µmol/L)	kg	26.46	21.52-31.83	26.03	20.69-32.92	0.556
ALMI (NH ₃ >50µmol/L)	kg/m ²	8.29	7.45-10.13	8.14	5.83-10.51	0.492

Anthropometric muscle parameters were not influenced by the intervention

After the three-month long intervention with LOLA, values of the whole cohort for mid arm circumference (MAC), mid arm muscle circumference (MAMC) and triceps skinfold thickness (for both arms individually) did not show a significantly change from T0 to T1 (Figure 11A-F).

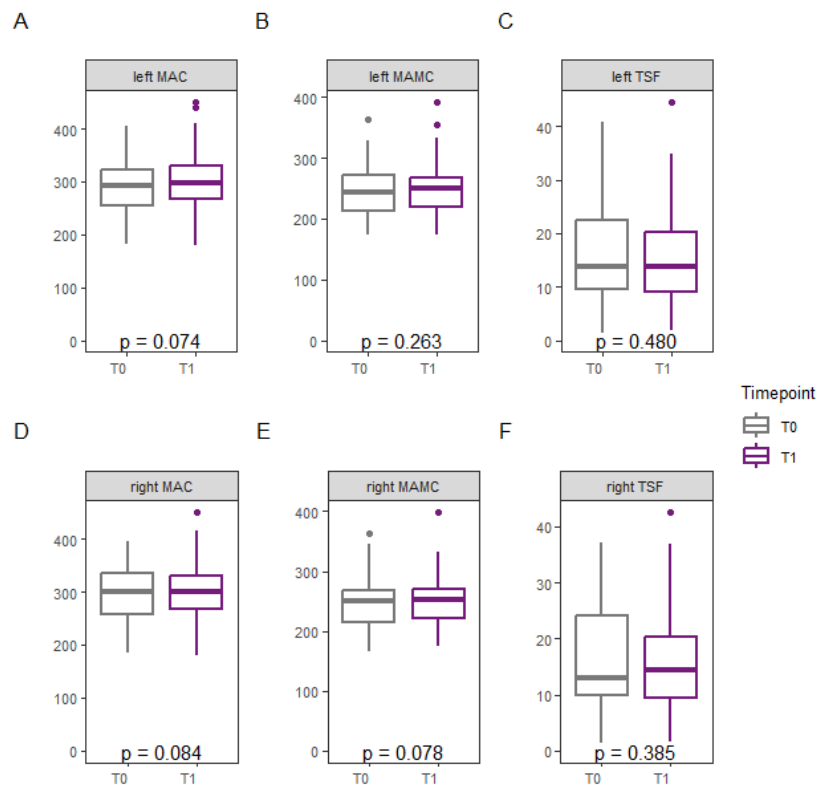


Figure 11: Muscle Parameters at T0 and T1: (A) left arm mid arm circumference [mm]; (B) left mid arm muscle circumference [mm]; (C) left triceps skinfold thickness (TSF); (D) right arm mid arm circumference [mm]; (E) right mid arm muscle circumference; [mm] (F) right triceps skinfold thickness (TSF). T0: baseline; T1: end of the intervention

Influence of LOLA on routine biochemistry

The following biochemistry parameters were significantly different between T0 and T1: fibrinogen concentrations increased from a median of 296 mg/dL (95% CI: 248-337) to 314 (95% CI: 262-351; $p = 0.037$; Figure 12A); glomerular filtration rate increased from a median of 91.66 mL/min (95% CI: 78.54-95.05) to 92.9 mL/min (95% CI: 85.19-99.67; $p = 0.005$; Figure 12B); gamma glutamyl transferase concentration increased from a median value of 108 U/L (95% CI: 70-158) to 114 U/L (95% CI: 75-196; $p = 0.03$; Figure 12C); creatinine concentration increased from a median of 0.79 mg/dL (95% CI: 0.75-0.88) to 0.78 mg/dL (95% CI: 0.69-0.86; $p = 0.009$; Figure 12D). Further details about measured blood parameters are shown in Table 4.

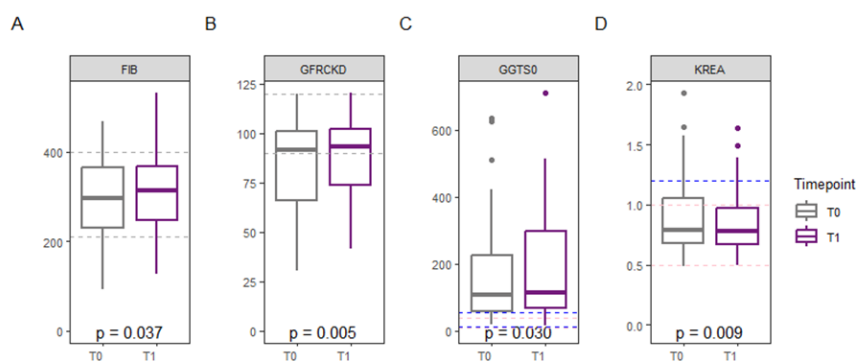


Figure 12: Blood parameters affected by the treatment with LOLA: (A) fibrinogen [mg/dL]; (B) Glomerular filtration rate [mL/min]; (C) Gamma-glutamyl transferase (GGTS0) [U/L]; (D) Creatinine (KREA) [mg/dL]. Dashed lines represent reference ranges: (pink depicts the normal range for females; blue for males). T0: baseline; T1: end of the intervention

Table 4: Routine Biochemistry parameters measured at T0 and T1.

Parameter	Unit	T0-Median (95% CI)	T1-Median (95% CI)	Normal Range (m/f)	p-value
Leukocytes	10 ⁹ /L	6.23 (4.96; 7.23)	5.81 (5.26; 7.07)	4.20 - 11.40	0.473
Erythrocytes	10 ¹² /L	4.17 (3.99; 4.37)	4.26 (4.10; 4.50)	4.10 - 5.75 / 3.90 - 5.15	0.701
Thrombocytes	10 ⁹ /L	141 (99; 178)	140.5 (107; 169)	140 - 440	0.678
Bilirubin	mg/dL	0.78 (0.57; 1.08)	0.84 (0.66; 1.13)	1.2	0.39
Aspartate aminotransferase (AST)	U/L	36 (33; 41)	37.5 (31; 49)	50/46	0.168
Alanine aminotransferase (ALT)	U/L	26 (23; 33)	28.5 (22; 38)	50/45	0.21
Gamma-glutamyl transferase (GGT)	U/L	108 (70; 158)	114 (75; 196)	55/38	0.03 *
Alkaline phosphatase	U/L	99.5 (90; 123)	112 (91; 125)	40-130 / 35-105	0.361
Creatinine	mg/dL	0.79 (0.75; 0.88)	0.78 (0.69; 0.86)	0.5-1.2 / 0.5-1	0.009 *
Glucose	mg/dL	100 (76; 140)	96 (78; 134)	70-100	0.544
Glomerular filtration rate (GFR)	mL/min	91.665 (78.54; 95.05)	92.9 (85.19; 99.67)	90.0 - 120.0	0.005 *
C-reactive protein (CRP)	mg/dL	3.1 (1.9; 3.8)	4.1 (2.2; 5.1)	5	0.074
Albumin	g/dL	4.1 (3.9; 4.3)	4.2 (4.1; 4.2)	3.5 - 5.5	0.238
Prothrombin- International Normalized Ratio (INR)		1.16 (1.08; 1.25)	1.12 (1.06; 1.27)	0.8 - 1.1	0.299
Ammonia	µmol/L	38 (31; 40)	34 (29; 39)	50	0.955
Fibrinogen	mg/dL	296 (248; 337)	314 (262; 351)	210 - 400	0.037 *
MELD		8.5 (7; 11)	8 (7; 11)		0.202
Child-Pugh Score		6 (6; 6)	6 (6; 6)		0.888

T0: baseline; T1: end of the intervention

Ammonia decreased in the whole cohort from 38 µmol/L (95% CI: 31-40) for T0 to 34 µmol/L (95% CI: 29-39; p = 0.955; Figure 13A), which did not reach statistical significance. Patients with ammonia concentrations above the upper limit of normal of 50 µmol/L at T0 (n=10; 9 males and one female) were investigated separately. In this subgroup a significant decrease in the ammonia concentrations from a median value of 69.5 µmol/L (95% CI: 54-225) to 46.0 µmol/L (95% CI: 22-66; p=0.004, Figure 13B) was observed.

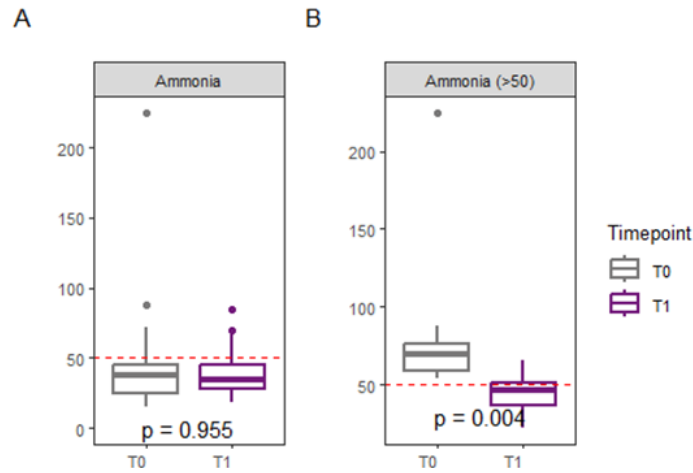


Figure 13: Ammonia concentration [µmol/L] at T0 and T1: (A) the whole cohort and (B) patients whose ammonia concentrations were above 50 µmol/L at T0 and T1.

Sarcopenia biomarkers were not affected by the intervention

Biomarkers related to sarcopenia (myostatin, FGF21, insulin like growth factor-1 and irisin) did not show a significant change from T0 to T1. Details can be found in Figure 14 and Table 5.

Table 5: Level of sarcopenia biomarkers at T0 to T1.

parameter	Unit	T0	95% CI	T1	95% CI	p-value
IGF1	ng/mL	40.1	32.4-50.5	42.55	32.8-52.0	0.88
myostatin	µg/mL	25.96	23.02-29.5	27.55	23.84-28.75	0.644
FGF21	pg/mL	249.81	163.2-429.12	270.01	159.41-495.09	0.981
Irisin	µg/mL	15.55	14.37-16.96	16.22	13.34-17.63	0.342

T0: baseline; T1: end of the intervention

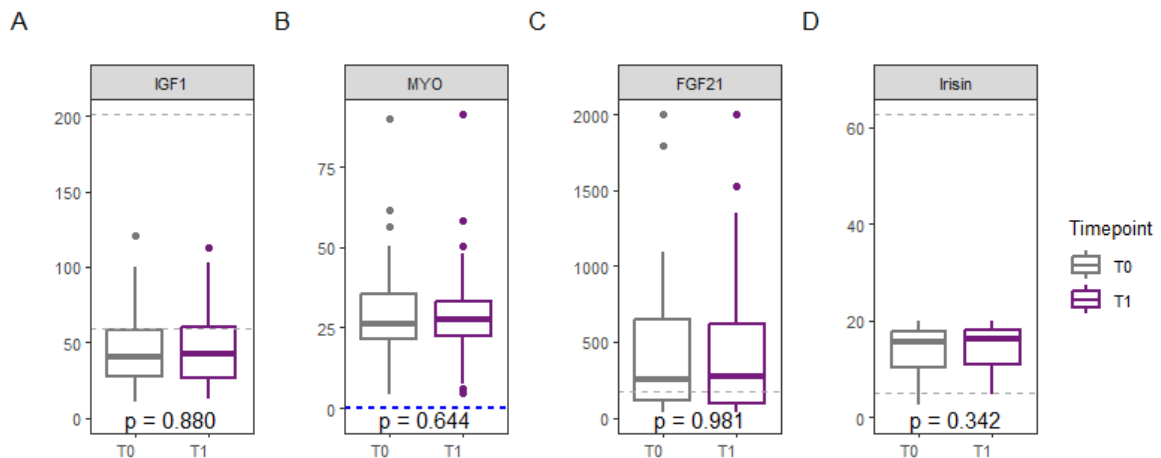


Figure 14: Concentrations of muscle biomarkers in serum at T0 and T1: (A); insulin-like growth factor-1 (IGF1) [ng/mL], (B) Myostatin [µg/mL], (C) fibroblast growth factor-21 (FGF21) [pg/mL], (D) Irisin [µg/mL]. Dashed lines represent reference medians / ranges according to the manufacturers. T0: baseline; T1: end of the intervention

LOLA intervention was associated with improvement of intestinal permeability and inflammatory response towards endotoxin

DAO, a serum marker of intestinal permeability, decreased significantly within the normal range from a median concentration of 12.75 U/mL (95% CI: 11.25-17.45) to a median concentration of 11.15 U/mL (95% CI: 9.9-15.65; p=0.016; Figure 15A). LBP concentrations increased significantly within the normal range from a median concentration of 17.05 µg/mg (95% CI: 14.7-19.8) to 17.39 µg/mg (95% CI: 16.2-21.9; p=0.006; Figure 15E). The other gut permeability biomarkers zonulin, calprotectin and sCD14 did not change significantly through the intervention with LOLA (Figure 15B-D, Table 6).

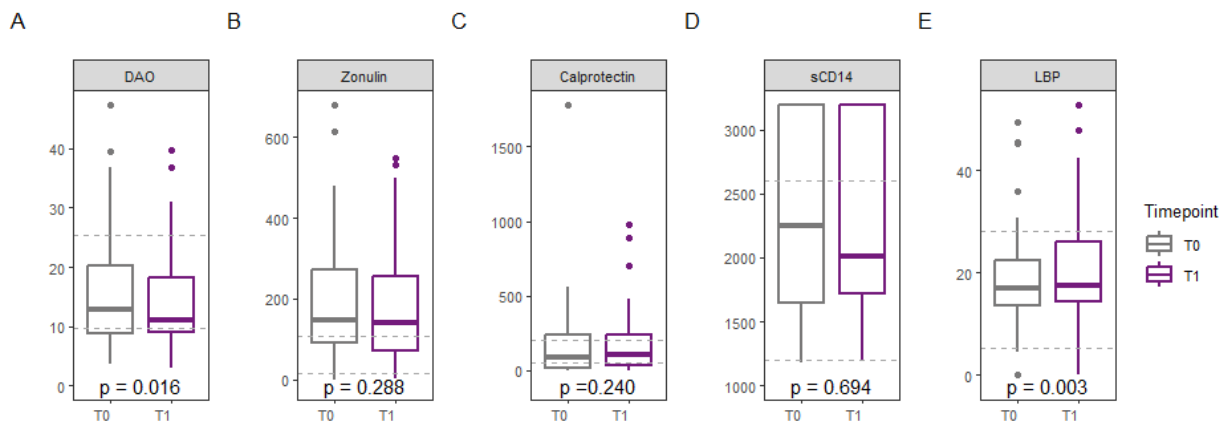


Figure 15: Concentrations of gut barrier and inflammation biomarkers in serum and stool at T0 and T1: (A) Diamino oxidase (DAO) in serum [U/mL], (B) zonulin [ng/mg], (C) calprotectin [µg/mg], (D) glycoprotein sCD14 [ng/mg], (E) LPS binding protein (LBP) [µg/mL]. Dashed lines represent reference medians / ranges according to the manufacturers T0: baseline; T1: end of the intervention

Table 6: Level of gut permeability and inflammation biomarkers at T0 and T1

parameter	Unit	T0	95% CI	T1	95% CI	p-value
DAO	U/mL	12.75	11.25-17.45	11.15	9.9-15.65	0.016
Zonulin	ng/mg	147	105-208	140.5	78-185	0.288
Calprotectin	µg/mg	84.03	29.9-196.93	104.14	67.08-203.4	0.240
sCD14	ng/mg	2253.97	1763.18-3200	2015.12	1818.52-3200	0.694
LBP	µg/mL	17.05	14.7-19.8	17.39	16.2-21.9	0.006

Table 7: Mean values of Biomarker concentrations, mean values of the normal range according to manufacturer’s instructions (sCD14, LBP, Zonulin), Calprotectin according to (54), DAO according to (9). T0 – baseline.

Biomarker	Unit	T0		Normal range	
		Mean	SD	Mean	SD
DAO	[U/ L]	15.5	9.6	16.1	6.7
Calprotectin	[µg/mg]	175.9	296.7	30.5	3.9
Zonulin	[ng/mg]	195.5	162.9	61	46
LBP	[µg/mg]	18.4	10	11.2	5.7
sCD14	[ng/mg]	2348.3	744.9	1900	546

LOLA intervention was associated with changes in serum, stool and urine metabolites

Metabolomic profiles were investigated across different sample types (serum (n=51), stool (n=48), and urine (n=38)) from the whole cohort for both T0 and T1. To assess overall metabolic variation between timepoints, principal component analysis (PCA) and permutational multivariate analysis of variance (PERMANOVA) for each serum, stool and urine were performed. While PCA plots showed minor degrees of separation between T0 and T1 (Figure 16A–C) without distinct clustering (suggesting modest global shifts in metabolite profiles), the results of the PERMANOVA indicated significant intervention-dependent variation across all sample types: serum ($R^2=0.85$, $F=5.83$, $p=0.001$), stool ($R^2=0.71$, $F=2.39$, $p=0.001$), and urine ($R^2=0.78$, $F=3.47$, $p=0.001$).

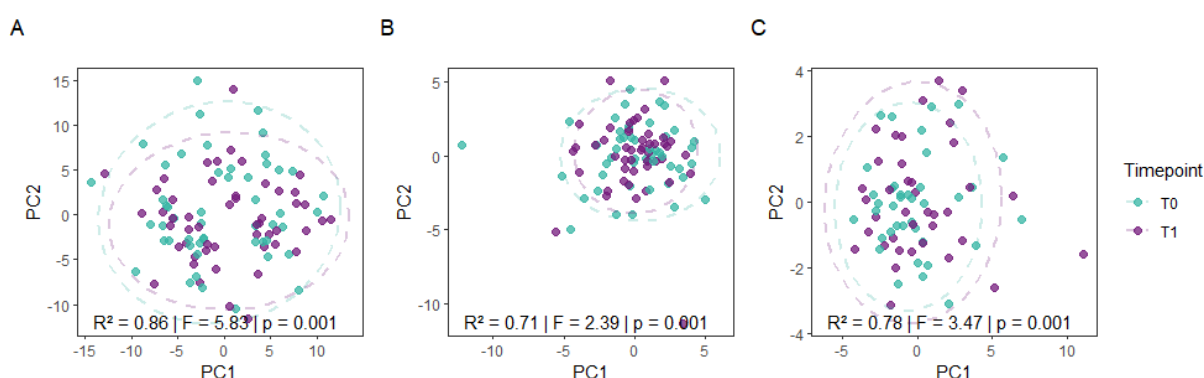


Figure 26: Principal Component Analysis (PCA) plots of (A) serum, (B) stool, and (C) urine samples for the whole cohort for samples at T0 and T1.

PLS-DA component plots were used to visually explore the separation of metabolite profiles between T0 and T1 across serum, stool, and urine samples. Clustering according to the timepoint was observed, suggesting metabolic changes throughout the intervention (Figures 17A-C). The first two PLS components explained a proportion of the variance in the metabolite data (22.8% and 8.6% in serum, 8.5% and 14.7% in stool, and 36.7% and 5.8% in urine, for components 1 and 2, respectively). Key metabolites contributing most to the observed separation were identified using VIP score plots. The top ten metabolites with VIP scores greater than 1 are shown in Figures 18A-C. In serum samples, the most influential metabolites included amino acids and lipoproteins, with alanine showing the highest VIP score. Stool samples revealed changes in a diverse set of compounds, including amino acids, sugars, organic acids, bile acids, and alcohols, with lysine ranking highest. In urine samples, top-ranking metabolites included amino acids, alkaloids, organic acids, and their derivatives. Notably, 9 out of the 10 most influential urinary metabolites showed increased abundance following the intervention.

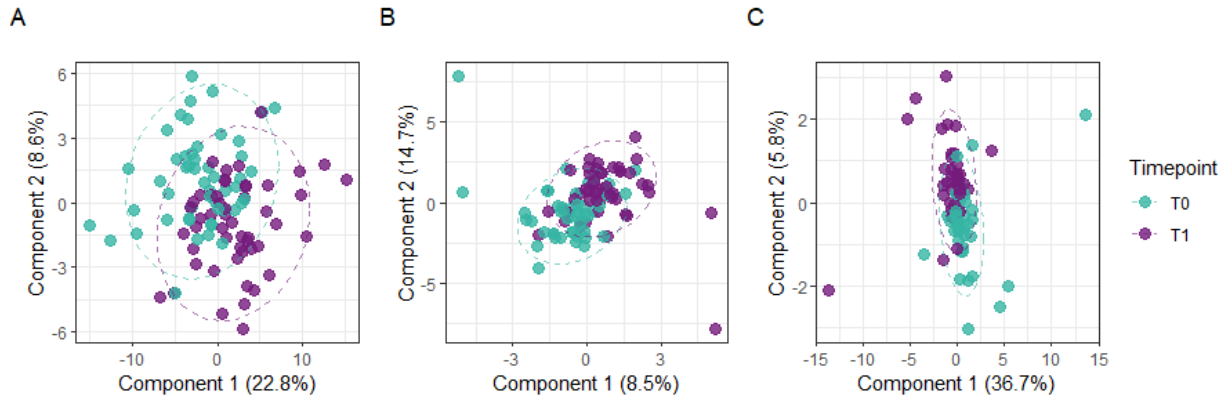


Figure 17: PLS-DA component plots to visualize partial separation of T0 and T1 samples for the whole cohort. (A) serum, (B) stool and (C) urine samples.

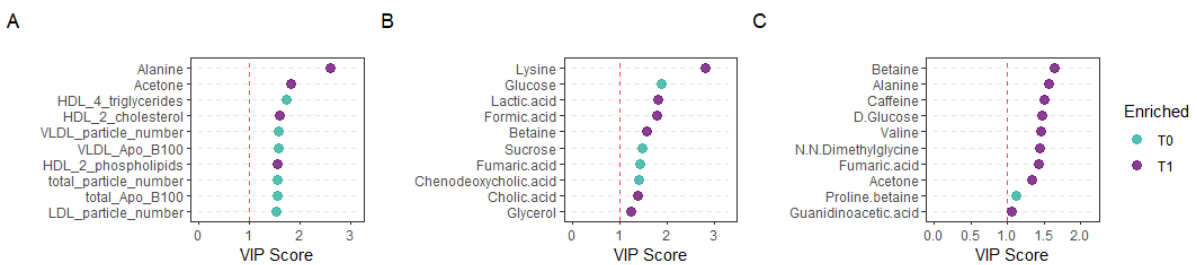


Figure 18: PLS-DA VIP score plots to visualize metabolites driving the group separation of T0 and T1 samples; Colours indicate the timepoints of metabolite enrichment in (A) serum, (B) stool, and (C) urine samples from the whole cohort.

Pathway enrichment analysis was performed using MetaboAnalyst to identify metabolic pathways impacted by the intervention. In serum samples from the whole cohort, no pathways remained statistically significant after FDR correction. However, selenocompound metabolism showed a significant change before correction ($p = 0.022$; Hits = 1; Expected = 0.991; FDR = 0.647). Additionally, several amino acids–related pathways, including those involving alanine, valine, leucine, isoleucine, tyrosine, glycine, serine, threonine, and phenylalanine, exhibited more observed hits than expected (Table 8). In stool and urine samples, no statistically significant enriched pathways were found. Nevertheless, within stool samples, elevated hit counts were observed in pathways associated with carbohydrate and amino acid metabolism, such as starch, sucrose, and galactose metabolism, as well as arginine, alanine, aspartate, and glutamate metabolism. Similarly in urine samples, pathways related to energy and amino acid metabolism —such as the TCA cycle, alanine, aspartate and glutamate metabolism, and glyoxylate metabolism — showed higher-than-expected hit counts, though none achieved statistical significance.

Table 8: Summary of pathway enrichment analysis for the whole cohort across serum, stool, and urine samples.

Sample Type	Metabolite Set	Total	Hits	Statistic	Expected	P value	Holm P	FDR
Serum	Selenocompound metabolism	20	1	5.111	0.990	0.022 *	0.648	0.648
	Pantothenate and CoA biosynthesis	20	1	2.608	0.990	0.105	1.000	0.908
	Alanine, aspartate and glutamate metabolism	28	3	1.946	0.990	0.129	1.000	0.908

	Valine, leucine and isoleucine degradation	39	2	1.714	0.990	0.177	1.000	0.908
	Valine, leucine and isoleucine biosynthesis	8	2	1.714	0.990	0.177	1.000	0.908
	Galactose metabolism	27	1	1.307	0.990	0.253	1.000	0.908
	Starch and sucrose metabolism	18	1	1.307	0.990	0.253	1.000	0.908
	Neomycin, kanamycin and gentamicin biosynthesis	2	1	1.307	0.990	0.253	1.000	0.908
	Citrate cycle (TCA cycle)	20	1	0.524	0.990	0.470	1.000	0.908
	Cysteine and methionine metabolism	33	1	0.524	0.990	0.470	1.000	0.908
	Arginine and proline metabolism	36	1	0.524	0.990	0.470	1.000	0.908
	Ubiquinone and other terpenoid-quinone biosynthesis	18	1	0.336	0.990	0.563	1.000	0.908
	Tyrosine metabolism	42	2	0.430	0.990	0.647	1.000	0.908
	Arginine biosynthesis	14	1	0.202	0.990	0.654	1.000	0.908
	Purine metabolism	70	1	0.202	0.990	0.654	1.000	0.908
	Pyrimidine metabolism	39	1	0.202	0.990	0.654	1.000	0.908
	Nitrogen metabolism	6	1	0.202	0.990	0.654	1.000	0.908
	Glycine, serine and threonine metabolism	33	2	0.274	0.990	0.745	1.000	0.908
	Lipoic acid metabolism	28	2	0.274	0.990	0.745	1.000	0.908
	Phenylalanine metabolism	8	2	0.228	0.990	0.756	1.000	0.908
Stool	Neomycin, kanamycin and gentamicin biosynthesis	2	1	1.441	1.053	0.244	1.000	0.962
	Tyrosine metabolism	42	2	0.741	1.053	0.437	1.000	0.962
	Lysine degradation	30	1	0.590	1.053	0.457	1.000	0.962
	Biotin metabolism	10	1	0.590	1.053	0.457	1.000	0.962
	Citrate cycle (TCA cycle)	20	2	0.804	1.053	0.468	1.000	0.962
	Starch and sucrose metabolism	18	3	0.655	1.053	0.481	1.000	0.962
	Ubiquinone and other terpenoid-quinone biosynthesis	18	1	0.447	1.053	0.517	1.000	0.962
	Taurine and hypotaurine metabolism	8	1	0.399	1.053	0.541	1.000	0.962
	Pyruvate metabolism	23	2	0.547	1.053	0.581	1.000	0.962
	Galactose metabolism	27	5	0.422	1.053	0.646	1.000	0.962
	Selenocompound metabolism	20	1	0.220	1.053	0.650	1.000	0.962
	Arginine biosynthesis	14	4	0.402	1.053	0.669	1.000	0.962
	Fatty acid biosynthesis	47	1	0.181	1.053	0.681	1.000	0.962
	Phenylalanine metabolism	8	2	0.253	1.053	0.682	1.000	0.962
	Phenylalanine, tyrosine and tryptophan biosynthesis	4	2	0.253	1.053	0.682	1.000	0.962
	Valine, leucine and isoleucine degradation	39	3	0.201	1.053	0.696	1.000	0.962
	Valine, leucine and isoleucine biosynthesis	8	3	0.201	1.053	0.696	1.000	0.962
	Butanoate metabolism	15	3	0.449	1.053	0.708	1.000	0.962
	Alanine, aspartate and glutamate metabolism	28	5	0.441	1.053	0.711	1.000	0.962
	Fructose and mannose metabolism	20	1	0.143	1.053	0.715	1.000	0.962
Urine	Galactose metabolism	27	1	2.605	1.333	0.164	1.000	0.709
	Starch and sucrose metabolism	18	1	2.605	1.333	0.164	1.000	0.709
	Neomycin, kanamycin and gentamicin biosynthesis	2	1	2.605	1.333	0.164	1.000	0.709
	Propanoate metabolism	21	1	0.292	1.333	0.643	1.000	0.933
	Butanoate metabolism	15	1	0.292	1.333	0.643	1.000	0.933
	D-Amino acid metabolism	15	1	0.076	1.333	0.813	1.000	0.933
	Selenocompound metabolism	20	1	0.072	1.333	0.818	1.000	0.933
	Citrate cycle (TCA cycle)	20	3	0.300	1.333	0.836	1.000	0.933
	Alanine, aspartate and glutamate metabolism	28	4	0.243	1.333	0.896	1.000	0.933
	Glycine, serine and threonine metabolism	33	1	0.020	1.333	0.905	1.000	0.933
	Glycolysis / Gluconeogenesis	26	2	0.096	1.333	0.920	1.000	0.933
	Pyruvate metabolism	23	2	0.096	1.333	0.920	1.000	0.933
	Glyoxylate and dicarboxylate metabolism	31	4	0.204	1.333	0.933	1.000	0.933

Associations between biomarkers, gut health, and clinical factors

To examine potential associations between appendicular skeletal muscle mass, bacterial biomarkers identified through LefSe analysis (*Enterococcus*, *Romboutia*), gut inflammation and permeability markers, and clinically relevant parameters influenced by the intervention (fibrinogen, creatinine, bilirubin, albumin, and international normalized ratio, CRP), a Spearman’s rank correlation analysis was conducted. Significant correlations are summarized in Table 9 and illustrated in Figure 19A. Additionally, to further investigate these associations, a correlation-based network (NW) was generated using Spearman’s rank correlation with a threshold of 0.3. The resulting network structure closely mirrors the correlation plot, emphasizing key interactions between biomarkers and clinical parameters, as shown in Figure 19B. Liver function clusters with inflammation and *Romboutia* and gut permeability also clusters with inflammation.

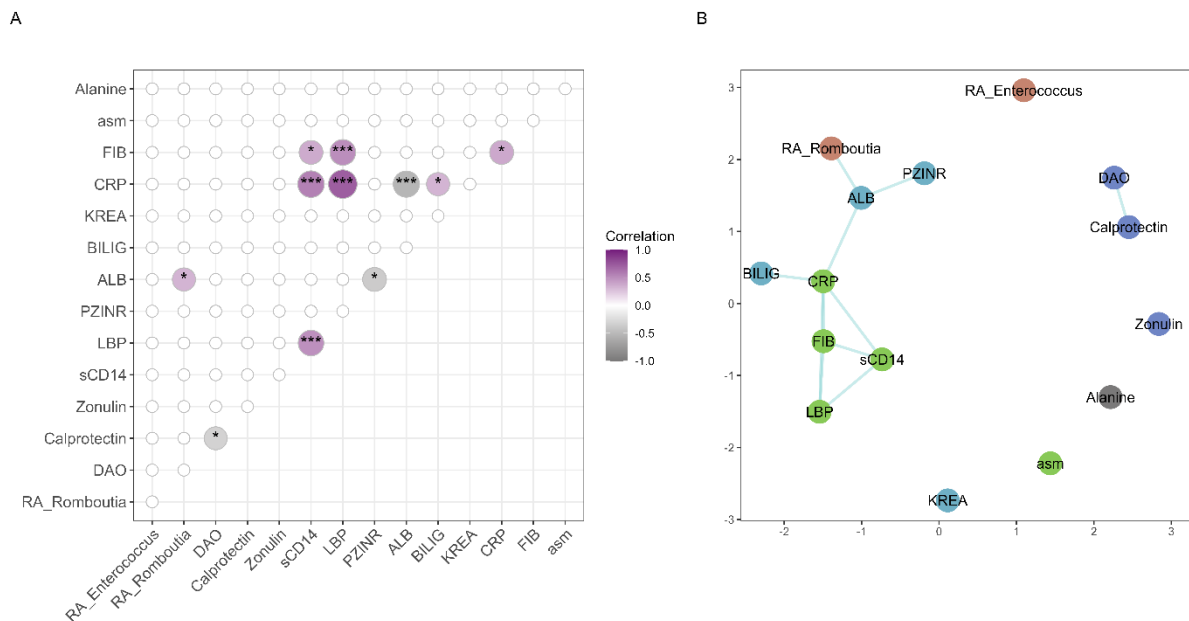


Figure 19: Correlations among relative abundance of bacterial biomarkers discovered through LefSe analysis (*Enterococcus*, *Romboutia*), gut inflammation and permeability markers (DAO, calprotectin, zonulin, LBP, sCD14), clinical parameters significantly affected by the intervention (bilirubin (BILIG), fibrinogen (FIB), c-reactive protein (CRP), creatinine (KREA), albumin (ALB), international normalized ratio (PZINR), serum-alanine). (A) correlation plot based on spearman rank correlation, (B) correlation-based network (using spearman rank correlation). T0: baseline; T1: end of the intervention

Table 9: Results of the spearman rank correlation analysis, correlation strength and significant relationships

Variables	Correlation	p-value	Significance
LBP sCD14	0.4918	<0.001	***
CRP sCD14	0.5588	<0.001	***
CRP LBP	0.7167	<0.001	***
FIB LBP	0.5033	<0.001	***
CRP ALB	-0.5300	<0.001	***
ALB RA_Romboutia	0.3252	0.021	*
Calprotectin DAO	-0.3199	0.047	*
Creatine_serum DAO	-0.3397	0.014	*

FIB	sCD14	0.3682	0.012	*
ALB	PZINR	-0.3696	0.011	*
CRP	BILIG	0.3319	0.030	*
FIB	CRP	0.3801	0.016	*

Safety and Adherence to LOLA

In total 42 adverse events were reported and of those. Thirty adverse events in 19 patients were classified as adverse events; most of them were gastrointestinal symptoms (n=15) and general symptoms (n=4, vertigo, fatigue, weakness), additionally skin irritations, joint pain, viral infections, and urological conditions were diagnosed during the study period. The gastrointestinal symptoms were judged to be possibly related to the study drug. Eleven adverse events in 9 patients were classified as serious adverse events, 5 were related to the underlying cirrhosis (acute kidney injury, hepatic encephalopathy, TIPS placement and 2 deaths due to decompensation of the liver cirrhosis that occurred after screening but before the first dose of the study drug. Furthermore, two diagnoses of inguinal hernia and one diagnosis of choledocholithiasis were made. One hospital admission because of new diagnosis of myasthenia gravis (symptom onset already before the start of the study drug) and one hospital admission because of preexisting depression and one diagnosis of cholangiocellular carcinoma (86 days after inclusion into the study). None of the severe adverse events was deemed related to the study product by the study physicians. Fifteen patients dropped out of the study: Two patients deceased in the period after screening prior to the start of the intervention due to decompensation of the liver cirrhosis; two had surgical intervention and did not start again to take LOLA; eight patients did not tolerate LOLA well; one patient stopped LOLA intake because the burden of the study was too high; one patient had to be excluded since baseline sampling was incomplete; one patient had to be excluded since adherence to the study product was below 50%. Adherence to the study product (LOLA) was measured by counting empty and unused sachets which were returned after the intervention. Patients that participated in the study took 90.5% (\pm 15.25%) median doses, as displayed in Figure 20.

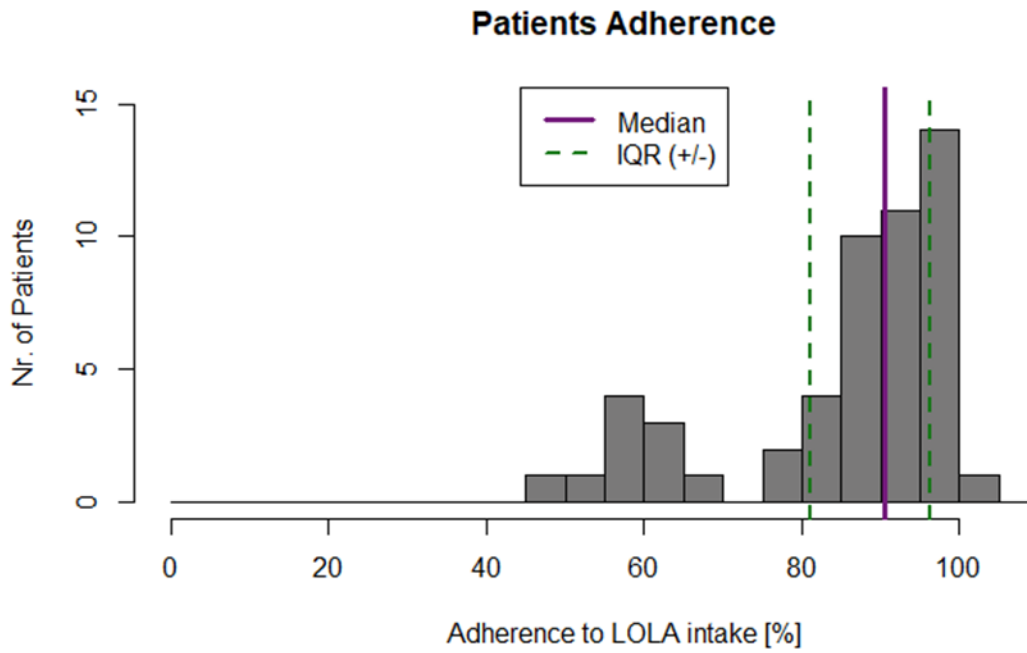


Figure 20: Histogram showing the adherence to the study product (LOLA) [%]; the blue line represents median adherence; green dotted lines the interquartile range. Patients with an adherence of <50% were defined as nonadherent and excluded (n=1). T0: baseline; T1: end of the intervention

Table 10: Documented adverse events: * Spontaneous bacterial peritonitis, hepatorenal syndrome, hepatic encephalopathy Grade (2); **Symptoms prior to T0; *** 1 elective and 1 emergency surgery due to incarcerated hernia.

Participants [n; %]	52 (100%)	MEDDRA code
AEs	30 in 19 patients (36.5%)	
Emesis	1	10014542
Diarrhea	7	10012735
Heartburn	1	10019326
Nausea	2	10028813
Abdominal discomfort	1	10000059
Flatulence	3	10016766
Vertigo	1	10047340
Fatigue	1	10016250
Weakness	1	10028372
Nervousness	1	10029216
Rash	1	10037844
Itching	1	10023084
Joint pain	2	10023222
Viral infection	2	10047461
Influenza	1	10016790

Nephrolithiasis	2	10029148
Benign prostata hyperplasia	1	10004446
Polyuria	1	10036142
SAEs		11 in 9 patients (17.3%)
Acute kidney failure	1	10000821
Hepatic encephalopathy stage 2	1	10085578
Transjugular intrahepatic portosystemic shunt placement	1	10068826
Death	2	10011906
Hernia inguinalis repair	2	10022020
Cholecystolithiasis	1	10008604
Preexisting depression requiring hospitalization	1	10054112
Myasthenia gravis	1	10028417
Cholangiocarcinoma	1	10008593

Subgroup analyses

High versus low baseline ammonia

To assess potential effects of serum ammonia concentration of patients on the relative abundance of bacterial biomarkers (*Flavonifractor* and *Oscillospira*), subgroups of patients with falling and increasing ammonia concentrations throughout the intervention period were formed. Patients with decreasing ammonia levels from T0 to T1 (n=21) showed a non-significant increase in the relative abundance of the genus *Oscillospira* (p=0.675) (Figure 21A) and a non-significant decrease in the genus *Flavonifractor* (p=0.49) (Figure 21B). The subgroup of patients with increasing ammonia concentrations throughout the intervention (n=24) showed a non-significant increase in the relative abundance of *Oscillospira* (p=0.477) (Figure 21C) and a non-significant decrease in the relative abundance of *Flavonifractor* (p=0.091) (Figure 21D).

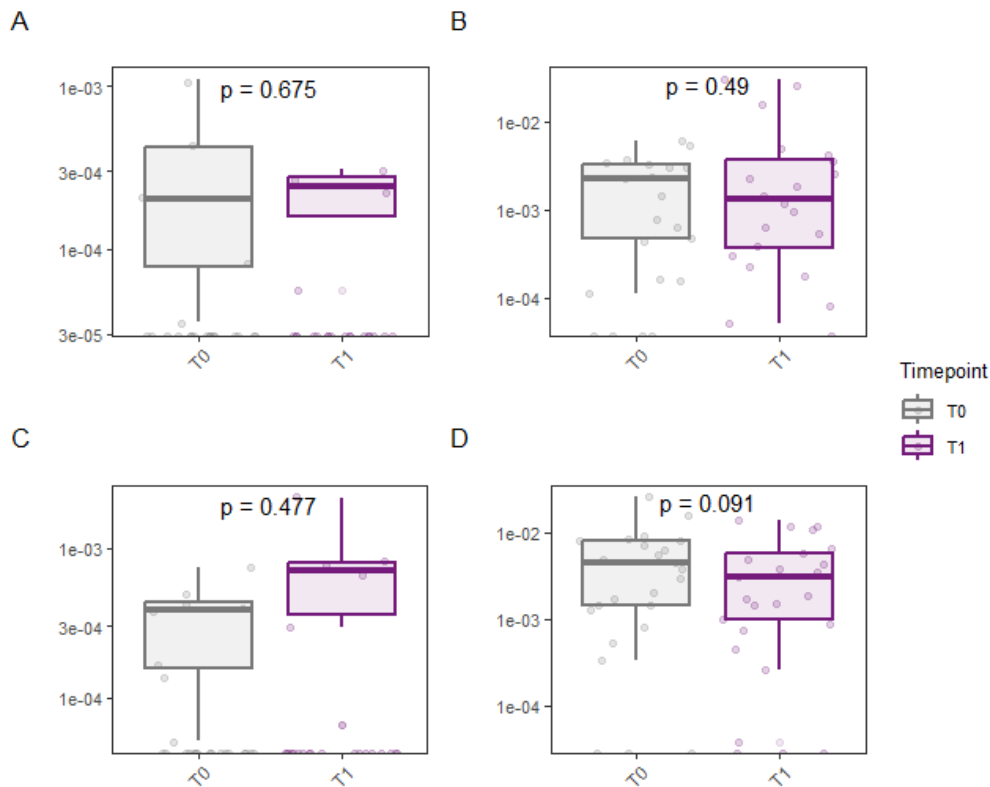


Figure 21: Relative abundance the bacterial genera *Oscillospira* and *Flavonifractor* at T0 and T1. (A) and (B) show the results for patients with falling ammonia values (n = 21) during the intervention, were *Oscillospira* occurs in 6 patients (T0: n=5; T1: n=4) and *Flavonifractor* occurs in 20 patients (T0: n=17; T1: n=20). (C) and (D) show the results for patients with rising ammonia values (n = 24) during the intervention were *Oscillospira* occurs in 9 patients (T0: n=8; T1: n=6); *Flavonifractor* occurs in 22 patients (T0: n=21; T1: n=21). T0: baseline; T1: end of the intervention

Gender differences

Alcohol use was more common and higher in male participants. Other parameters were comparable between men and woman. Within the subgroup of female patients (n=21) four parameters were significantly altered after the intervention. The median values the SF-36 item mental health was

significantly reduced from 68% (95% CI: 56-84) to 52% (95% CI: 44-80; $p=0.018$, Figure 22A). The MELD score decreased from a median value of 8 (95% CI: 7-13) to 7 (95% CI: 6-10; $p=0.015$; Figure 22B). Corresponding, the prothrombin time increased from a median of 76% (95% CI: 65-88) to 86% (95% CI: 66-99; $p < 0.001$; Figure 22C) and the prothrombin international normalized ratio (INR) decreased from a median of 1.16 (95% CI: 1.07-1.28) to 1.09 (95% CI: 1.00-1.27; $p = 0.005$; Figure 22D).

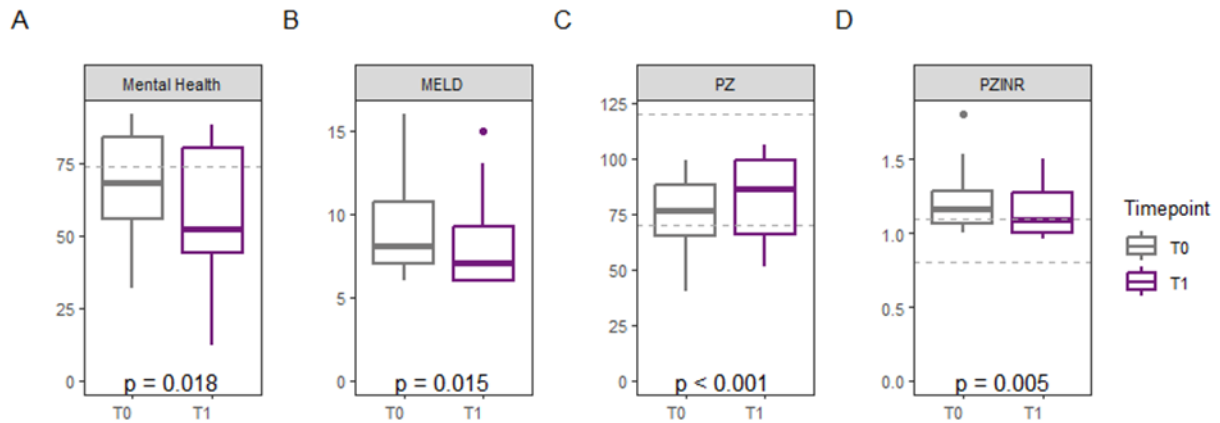


Figure 22: Significantly altered parameters in female participants: (A) SF36-mental health [%]; (B) Model of end stage liver disease; (C) Prothrombin time [%] and (D) Prothrombin-international Normalized Ratio (INR). T0: baseline; T1: end of the intervention

Within male patients ($n=31$), eight parameters were significantly altered after the intervention. Appendicular skeletal muscle mass declined from a median of 25150 g (95% CI: 22417–27539) to 24864 g (95% CI: 19993–27172; $p=0.021$; Figure 23A). Similarly, ammonia levels decreased from a median of 39 $\mu\text{mol/L}$ (95% CI: 33–45) to 34 $\mu\text{mol/L}$ (95% CI: 29–40; $p=0.047$; Figure 23B). The SF-36 item Vitality increased over the study period from a median value of 45% (95% CI: 35-70) to a median value of 60% (95% CI: 45-75; $p=0.003$; Figure 23C). Transaminases increased significantly, with alanine aminotransferase rising from 27 U/L (95% CI: 23–36) to 30 U/L (95% CI: 26–43; $p=0.022$; Figure 23D), and aspartate aminotransferase increasing from 38 U/L (95% CI: 33–45) to 44 U/L (95% CI: 31–57; $p=0.037$; Figure 23E). The inflammatory marker CRP increased from 2.7 mg/dL (95% CI: 1.4–3.9) to 4.5 mg/dL (95% CI: 2.1–6.4; $p=0.037$; Figure 23F), and changes in kidney function were observed, with glomerular filtration rate increasing from 97.02 mL/min (95% CI: 82.61–102.85) to 99.26 mL/min (95% CI: 89.52–103.38; $p=0.035$; Figure 23G). Creatinine increased slightly from 0.8 mg/dL (95% CI: 0.69–0.93) to 0.81 $\mu\text{mol/L}$ (95% CI: 0.68–0.91; $p=0.033$; Figure 23H).

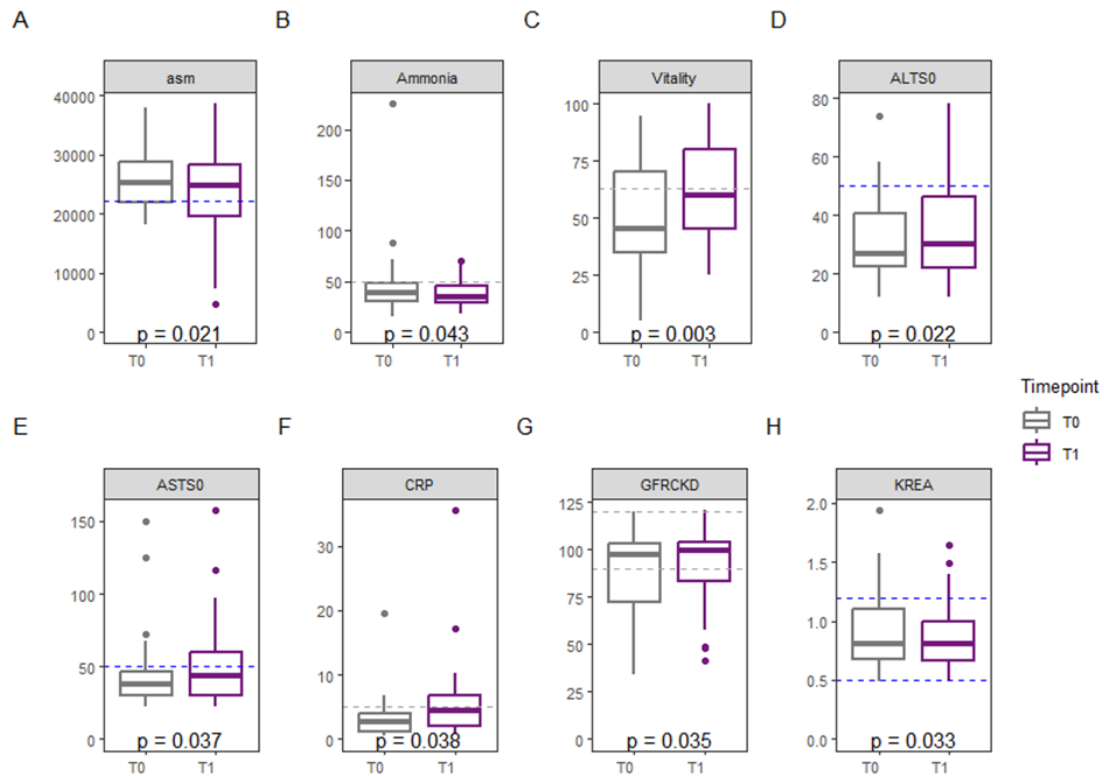


Figure 23: Significant altered parameters in male participants: (A) appendicular skeletal muscle mass [g]; (B) Ammonia [$\mu\text{mol/L}$]; (C) SF36-Vitality [%]; (D) Alanine aminotransferase [U/L]; (E) Aspartate aminotransferase [U/L]; (F) CRP [mg/dL]; (G) glomerular filtration rate [mL/min] and (H) creatinine [mg/dL]. T0: baseline; T1: end of the intervention

Discussion

We conducted an open-label phase 4 study to understand whether LOLA, in addition to its long-proven ammonia lowering and hepatic encephalopathy improving effect, can also influence the gut microbiome and quality of life. LOLA improved the quality-of-life aspect vitality in patients with cirrhosis. LOLA further improved some aspects of liver disease severity and may be useful to prevent muscle loss in patients with elevated ammonia levels. LOLA slightly altered microbiome composition without measurable functional impact and improved biomarkers of intestinal barrier and lipopolysaccharide binding.

Our hypothesis that LOLA could influence the composition of the gut microbiome was generated based on a retrospective study, where we could show in a propensity score matched cross-sectional study, that LOLA intake was associated with higher abundance of the potentially beneficial genera *Flavonifractor* and *Oscillospira* (21). In a rat model of steatotic liver disease, LOLA induced an increase in abundance of *Helicobacter rodentium*, *Parabacteroides goldsteinii*, and *Parabacteroides distasonis* as well as changes in some related metabolic pathways. (55) The authors interpreted these changes as positive, since these bacteria have been proposed as next generation probiotics with beneficial effects in preventing and treating inflammation and obesity. (55) Both our own previous study and the rat study did not observe any effects of LOLA on alpha and beta diversity (21,55). In the current

prospective study, no effect on alpha and beta diversity was observed, strengthening the assumption that LOLA does not interfere with overall microbiome structure, which can be considered as an important safety aspect for long-term use. Furthermore, no effect on our target genera *Flavonifractor* and *Oscillospira* was found. Our result may be explained by the treatment duration, which was up to 29 months in our retrospective study and 28 weeks in the animal study but only 12 weeks in the study we present here. An additional biomarker search revealed that the genus *Romboutsia* was significantly reduced at the end of the treatment period whereas the genus *Enterococcus* was significantly enriched. *Romboutsia* was isolated from rat feces (56) and so far only described in two studies in cirrhosis: A higher abundance was associated with reduced visceral fat in sarcopenia and a lower abundance was observed with gluten free diet in patients with primary sclerosing cholangitis and colitis (57,58). *Romboutsia* may alleviate intestinal inflammation according to animal data (59). The genus *Enterococcus* has commonly been associated with liver cirrhosis (60), where this genus seems to increase with increasing disease severity (61) and complications, such as HE (62) and a higher risk for hospitalization. (63) Pathophysiologically, the overgrowth of *Enterococcus* was linked to gastric acid suppression in alcoholic liver disease (64). However, within the genus *Enterococcus*, different species can be found, some with pathogenic potential and some with beneficial functions. (65) Immunomodulatory, metabolic and antimicrobial effects have been described in humans and animals. (66) Since our cohort showed stable and, in some aspects, even improving liver function and given the limitation of resolution below genus level of 16s rDNA sequencing, it is not possible to draw a firm conclusion whether our observed increase in *Enterococcus* is a sign of the natural history of the liver disease or a reaction to the intervention.

While predicted microbiome function analysis showed that LOLA was only associated with minor changes by slightly altering selenocompound metabolism, metabolomics analysis, which can be considered the more direct measure of microbiome and host function, revealed that the intervention with LOLA was associated with significant intervention-dependent metabolomic variation across all sample types. The strongest change was an increase in alanine, with several other, less strong and less consistent, amino acid and lipoprotein associated changes. These alterations most likely related to the intervention as we also observed in our previous retrospective study (21) and especially the finding in alanine increase was also found with LOLA treatment in a rat model of acute liver failure (67). The increase in alanine may be explained by stimulation of glutamine synthetase through LOLA (68), consequently leading to higher alanine synthetase. A reduction in serum alanine levels as well as a reduction in selenocompound metabolism was observed in liver cirrhosis patients with sarcopenia, compared to those without sarcopenia, indicating that LOLA may be able to improve sarcopenia associated metabolic pathways in cirrhosis (69). The alterations in serum lipids warrant further

consideration. Patients with liver cirrhosis show abnormalities in HDL particle composition and function and are increasingly suggested as novel biomarkers for liver disease severity and risk of complications (70,71). These changes were mainly observed in the group of patients with elevated ammonia levels at baseline, indicating that this group would benefit most from the intervention. Changes in mannose and glucose may be attributable to changes in nutrition of the participants. 15 participants with diabetes were included, possibly explaining the variation in glucose values. Pathway analysis revealed the strongest change in selenocompound metabolism as well as in different amino acid related pathways. Taken together, our metabolomics analysis shows on the one hand, that the intake of LOLA influences the concentrations of amino acids. In addition, the analysis also revealed changes beyond amino acids.

We further observed a slight improvement in intestinal permeability as measured by a significant decrease in DAO, a biomarker of impaired intestinal permeability in cirrhosis (72–75), as well as in increase in LBP within the normal range after the intervention. The significance of LBP modulation in cirrhosis may be considered controversial, since elevated levels of LBP could on the one hand be a biomarker of endotoxemia and inflammation, associated with complications and poor prognosis in cirrhosis and on the other hand, a vital first-line defense mechanism of the innate immune system, that has been associated with better outcome in patients with sepsis and cirrhosis (76–83). We interpret a rise of LBP within the normal range as a beneficial effect, since it can be considered as a sign of improved handling of lipopolysaccharide and lipopolysaccharide is one of the causal factors to impair innate immunity in cirrhosis (84,85). Experimental reduction of lipopolysaccharide was associated with improved function of neutrophil granulocytes (86).

LOLA treatment had several additional positive effects in our study. The clinically most relevant effect was the improvement in the aspect of vitality assessed by the SF36 quality of life score. Consistent with data from literature, we could confirm that all aspects of quality of life were significantly reduced in our cohort of patients with liver cirrhosis and minimal HE (87–89). Hepatic encephalopathy, even when minimal, is one of the key factors that affect quality of life of patients and caregivers (90–92). LOLA has been previously shown to improve health related quality of life, especially fatigue, sleep quality and concentration deficits in an open-label, prospective, multi-centre observational study in Germany (93). In a small randomized, placebo controlled study, that was only published as abstract so far, LOLA over 12 weeks led to increased energy levels and concentration (94) Out post hoc subgroup analysis revealed that the effect on vitality was most prominent in male participants. Further studies are warranted to clarify gender-specific effects. Besides the improvement in vitality, we also observed some promising changes in biochemistry. As expected, and shown consistently in previous trials, ammonia levels improved in those who had elevated ammonia levels at baseline (95–98). We also

observed a small but statistically significant increase in GGT levels, which may be explained by ongoing alcohol consumption in 15% of the subjects. Creatinine and glomerular filtration rate decreased, and fibrinogen increased. The change in creatinine and GFR could be interpreted as an improvement in renal function but also as a sign of ongoing muscle loss, that could not be stopped by LOLA (99). The increase in fibrinogen, that is produced in the liver, on the other hand, could point towards an improvement in liver function. While in the whole cohort, no change in MELD or Child-Pugh score was observed, MELD score improved significantly in women, mainly due to an improvement in prothrombin time/INR.

Our secondary hypothesis was, that LOLA could positively influence muscle mass in cirrhosis, based on the knowledge that a reduction of ammonia, which is a driver of sarcopenia, can improve protein synthesis and function (100). This hypothesis was also strengthened by data from an animal model of portal hypertension, where ammonia lowering with LOLA and rifaximin improved the muscle phenotype and function (101). While LOLA could not prevent muscle loss in the whole cohort, the subgroup of patients with elevated ammonia levels at baseline showed no decline in muscle mass. No changes were observed in muscle function assessments, liver frailty score, SARC-F, Barthel ADL index and muscle biomarkers. In the subgroup of patients with elevated ammonia levels at baseline, we also observed stronger differences in metabolomics composition, especially in serum, indicating that this group should be the target group for further investigations of effects of LOLA beyond ammonia lowering.

Our study is limited by the open label design that might bias subjective endpoints. The lack of statistically significant changes in our primary endpoint, the *Flavonifractor* and *Oscillospira* abundance may be due to the shorter duration of intervention in the prospective study compared to the retrospective data analysis, since the sample size calculation was based on this retrospective analysis.

Conclusion

In conclusion, our study showed that a short period of oral LOLA intake could not alter *Flavonifractor* and *Oscillospira* abundance of the gut microbiome but improved liver function biochemistry, vitality, intestinal permeability, reduced *Romboutsia* abundance and increased lipopolysaccharide handling. Muscle loss was prevented in the subgroup of patients with elevated ammonia levels and treatment related metabolomic changes were observed. LOLA therefore should be further tested as a treatment option beyond influencing ammonia metabolism.

Data availability

Sequencing data are available at the NCBI SRA (<https://www.ncbi.nlm.nih.gov/sra>) under the accession number PRJNA1223152.

References

1. Pimpin L. HEPAAHEALTH Project Report [Internet]. Geneva, Switzerland: European Association for the study of the liver; 2018 [cited 2024 Dec 4]. Available from: <https://easl.eu/publication/hepahealth-project-report/>
2. Gu W, Hortlik H, Erasmus HP, Schaaf L, Zeleke Y, Uschner FE, et al. Trends and the course of liver cirrhosis and its complications in Germany: Nationwide population-based study (2005 to 2018). *Lancet Reg Health Eur.* 2022 Jan;12:100240.
3. Gustot T, Stadlbauer V, Laleman W, Alessandria C, Thursz M. Transition to decompensation and acute-on-chronic liver failure: Role of predisposing factors and precipitating events. *J Hepatol.* 2021 Jul;75 Suppl 1:S36–48.
4. Qin N, Yang F, Li A, Prifti E, Chen Y, Shao L, et al. Alterations of the human gut microbiome in liver cirrhosis. *Nature.* 2014 Sep 4;513(7516):59–64.
5. Stadlbauer V, Komarova I, Klymiuk I, Durdevic M, Reisinger A, Blesl A, et al. Disease severity and proton pump inhibitor use impact strongest on faecal microbiome composition in liver cirrhosis. *Liver Int.* 2020 Apr;40(4):866–77.
6. Tripathi A, Debelius J, Brenner DA, Karin M, Loomba R, Schnabl B, et al. The gut-liver axis and the intersection with the microbiome. *Nat Rev Gastroenterol Hepatol.* 2018 Jul;15(7):397–411.
7. Maier L, Pruteanu M, Kuhn M, Zeller G, Telzerow A, Anderson EE, et al. Extensive impact of non-antibiotic drugs on human gut bacteria. *Nature.* 2018 Mar 29;555(7698):623–8.
8. Horvath A, Rainer F, Bashir M, Leber B, Schmerboeck B, Klymiuk I, et al. Biomarkers for oralization during long-term proton pump inhibitor therapy predict survival in cirrhosis. *Sci Rep.* 2019 Aug 19;9(1):12000.
9. Horvath A, Leber B, Schmerboeck B, Tawdrous M, Zettel G, Hartl A, et al. Randomised clinical trial: the effects of a multispecies probiotic vs. placebo on innate immune function, bacterial translocation and gut permeability in patients with cirrhosis. *Aliment Pharmacol Ther.* 2016 Nov;44(9):926–35.
10. Horvath A, Durdevic M, Leber B, di Vora K, Rainer F, Krones E, et al. Changes in the Intestinal Microbiome during a Multispecies Probiotic Intervention in Compensated Cirrhosis. *Nutrients.* 2020 Jun 23;12(6):1874.
11. Horvath A, Leber B, Feldbacher N, Steinwender M, Komarova I, Rainer F, et al. The effects of a multispecies synbiotic on microbiome-related side effects of long-term proton pump inhibitor use: A pilot study. *Sci Rep.* 2020 Feb 17;10(1):2723.
12. Horvath A, Leber B, Feldbacher N, Tripolt N, Rainer F, Blesl A, et al. Effects of a multispecies synbiotic on glucose metabolism, lipid marker, gut microbiome composition, gut permeability, and quality of life in diabetes: a randomized, double-blind, placebo-controlled pilot study. *Eur J Nutr.* 2020 Oct;59(7):2969–83.
13. Poo JL, Góngora J, Sánchez-Avila F, Aguilar-Castillo S, García-Ramos G, Fernández-Zertuche M, et al. Efficacy of oral L-ornithine-L-aspartate in cirrhotic patients with hyperammonemic hepatic encephalopathy. Results of a randomized, lactulose-controlled study. *Ann Hepatol.* 2006;5(4):281–8.

14. European Association for the Study of the Liver. Electronic address: easloffice@easloffice.eu, European Association for the Study of the Liver. EASL Clinical Practice Guidelines on nutrition in chronic liver disease. *J Hepatol*. 2019 Jan;70(1):172–93.
15. Olde Damink SWM, Jalan R, Dejong CHC. Interorgan ammonia trafficking in liver disease. *Metab Brain Dis*. 2009 Mar;24(1):169–81.
16. Wijdicks EFM. Hepatic Encephalopathy. *N Engl J Med*. 2016 Oct 27;375(17):1660–70.
17. Butterworth RF. Role of circulating neurotoxins in the pathogenesis of hepatic encephalopathy: potential for improvement following their removal by liver assist devices. *Liver Int*. 2003;23 Suppl 3:5–9.
18. Butterworth RF. Hepatic encephalopathy in alcoholic cirrhosis. *Handb Clin Neurol*. 2014;125:589–602.
19. Goh ET, Stokes CS, Sidhu SS, Vilstrup H, Gluud LL, Morgan MY. L-ornithine L-aspartate for prevention and treatment of hepatic encephalopathy in people with cirrhosis. *Cochrane Database Syst Rev*. 2018 May 15;5(5):CD012410.
20. Kircheis G, Lüth S. Pharmacokinetic and Pharmacodynamic Properties of L-Ornithine L-Aspartate (LOLA) in Hepatic Encephalopathy. *Drugs*. 2019 Feb;79(Suppl 1):23–9.
21. Horvath A, Traub J, Aliwa B, Bourgeois B, Madl T, Stadlbauer V. Oral Intake of L-Ornithine-L-Aspartate Is Associated with Distinct Microbiome and Metabolome Changes in Cirrhosis. *Nutrients*. 2022 Feb 10;14(4):748.
22. Bolyen E, Rideout JR, Dillon MR, Bokulich NA, Abnet CC, Al-Ghalith GA, et al. Reproducible, interactive, scalable and extensible microbiome data science using QIIME 2. *Nat Biotechnol*. 2019 Aug;37(8):852–7.
23. Ware JE, Sherbourne CD. The MOS 36-item short-form health survey (SF-36). I. Conceptual framework and item selection. *Med Care*. 1992 Jun;30(6):473–83.
24. Mahoney FI, Barthel DW. FUNCTIONAL EVALUATION: THE BARTHEL INDEX. *Md State Med J*. 1965 Feb;14:61–5.
25. Bullinger M, Kirchberger I. SF-36 Fragebogen zum Gesundheitszustand Handanweisung. Goettingen; 1998.
26. Malmstrom TK, Morley JE. SARC-F: a simple questionnaire to rapidly diagnose sarcopenia. *J Am Med Dir Assoc*. 2013 Aug;14(8):531–2.
27. Roberts HC, Denison HJ, Martin HJ, Patel HP, Syddall H, Cooper C, et al. A review of the measurement of grip strength in clinical and epidemiological studies: towards a standardised approach. *Age Ageing*. 2011 Jul;40(4):423–9.
28. Cooper C, Fielding R, Visser M, van Loon LJ, Rolland Y, Orwoll E, et al. Tools in the assessment of sarcopenia. *Calcif Tissue Int*. 2013 Sep;93(3):201–10.
29. Lai JC, Covinsky KE, Dodge JL, Boscardin WJ, Segev DL, Roberts JP, et al. Development of a novel frailty index to predict mortality in patients with end-stage liver disease. *Hepatology*. 2017 Aug;66(2):564–74.

30. Tang AM, Chung M, Dong KR, Bahwere P, Bose K, Chakraborty R, et al. Determining a global mid-upper arm circumference cut-off to assess underweight in adults (men and non-pregnant women). *Public Health Nutr.* 2020 Dec;23(17):3104–13.
31. Schweighofer N, Colantonio C, Haudum CW, Hutz B, Kolesnik E, Mursic I, et al. DXA-Derived Indices in the Characterisation of Sarcopenia. *Nutrients.* 2021 Dec 31;14(1):186.
32. Cruz-Jentoft AJ, Bahat G, Bauer J, Boirie Y, Bruyère O, Cederholm T, et al. Sarcopenia: revised European consensus on definition and diagnosis. *Age Ageing.* 2019 Jan;48(1):16–31.
33. Lafzi N, Altinkaynak M, Goksoy Y, Tor YB, Akpınar TS, Erten SN, et al. Estimation of the appendicular skeletal muscle mass and phase angle cut-off values from a young Turkish reference population using multifrequency bioelectrical impedance analysis. *Eur Rev Med Pharmacol Sci.* 2024 Feb;28(4):1282–8.
34. Kirk B, Bani Hassan E, Brennan-Olsen S, Vogrin S, Bird S, Zanker J, et al. Body composition reference ranges in community-dwelling adults using dual-energy X-ray absorptiometry: the Australian Body Composition (ABC) Study. *J Cachexia Sarcopenia Muscle.* 2021 Aug;12(4):880–90.
35. Lai JC, Covinsky KE, McCulloch CE, Feng S. The Liver Frailty Index Improves Mortality Prediction of the Subjective Clinician Assessment in Patients With Cirrhosis. *Am J Gastroenterol.* 2018 Feb;113(2):235–42.
36. Horvath A, Habisch H, Prietl B, Pfeifer V, Balazs I, Kovacs G, et al. Alteration of the Gut–Lung Axis After Severe COVID-19 Infection and Modulation Through Probiotics: A Randomized, Controlled Pilot Study. *Nutrients.* 2024 Jan;16(22):3840.
37. R: The R Project for Statistical Computing [Internet]. [cited 2024 Nov 13]. Available from: <https://www.r-project.org/>
38. Wei R, Wang J, Su M, Jia E, Chen S, Chen T, et al. Missing Value Imputation Approach for Mass Spectrometry-based Metabolomics Data. *Sci Rep.* 2018 Jan 12;8(1):663.
39. Lazar C, Burger T, Wieczorek S. imputeLCMD: A Collection of Methods for Left-Censored Missing Data Imputation [Internet]. 2022 [cited 2025 Apr 16]. Available from: <https://cran.r-project.org/web/packages/imputeLCMD/index.html>
40. R Core Team. R: A Language and Environment for Statistical Computing [Internet]. 2024 [cited 2024 Nov 22]. Available from: <https://www.r-project.org/>
41. Signorell A, Aho K, Alfons A, Anderegg N, Aragon T, Arachchige C, et al. DescTools: Tools for Descriptive Statistics [Internet]. 2024 [cited 2024 Nov 22]. Available from: <https://cran.r-project.org/web/packages/DescTools/index.html>
42. Wickham H. ggplot2: Elegant Graphics for Data Analysis [Internet]. 2016 [cited 2024 Nov 22]. Available from: <https://ggplot2.tidyverse.org/>
43. Bisanz J. jbisanz/qiime2R [Internet]. 2024 [cited 2024 Nov 22]. Available from: <https://github.com/jbisanz/qiime2R>
44. Davis NM, Proctor DM, Holmes SP, Relman DA, Callahan BJ. Simple statistical identification and removal of contaminant sequences in marker-gene and metagenomics data. *Microbiome.* 2018 Dec 17;6(1):226.
45. McMurdie PJ, Holmes S. phyloseq: an R package for reproducible interactive analysis and graphics of microbiome census data. *PLoS One.* 2013;8(4):e61217.

46. Borman T, Ernst FGM, Shetty SA, Lahti L. mia: Microbiome analysis. 2024 [cited 2024 Nov 22]. mia: Microbiome analysis. Available from: <https://github.com/microbiome/mia>
47. Battaglia T. btools: A suite of R function for all types of microbial diversity analyses [Internet]. 2024 [cited 2024 Nov 22]. Available from: <https://github.com/twbattaglia/btools>
48. Oksanen J, Simpson GL, Blanchet FG, Kindt R, Legendre P, Minchin PR, et al. vegan: Community Ecology Package [Internet]. 2024 [cited 2024 Nov 22]. Available from: <https://cran.r-project.org/web/packages/vegan/index.html>
49. Cao Y, Dong Q, Wang D, Zhang P, Liu Y, Niu C. microbiomeMarker: an R/Bioconductor package for microbiome marker identification and visualization. *Bioinformatics*. 2022 Aug 10;38(16):4027–9.
50. Mallick H, Rahnavard A, McIver LJ, Ma S, Zhang Y, Nguyen LH, et al. Multivariable association discovery in population-scale meta-omics studies. *PLoS Comput Biol*. 2021 Nov;17(11):e1009442.
51. Lu Y, Zhou G, Ewald J, Pang Z, Shiri T, Xia J. MicrobiomeAnalyst 2.0: comprehensive statistical, functional and integrative analysis of microbiome data. *Nucleic Acids Research*. 2023 Jul 5;51(W1):W310–8.
52. Rohart F, Gautier B, Singh A, Lê Cao KA. mixOmics: An R package for 'omics feature selection and multiple data integration. *PLoS Comput Biol*. 2017 Nov;13(11):e1005752.
53. Pang Z, Lu Y, Zhou G, Hui F, Xu L, Viau C, et al. MetaboAnalyst 6.0: towards a unified platform for metabolomics data processing, analysis and interpretation. *Nucleic Acids Res*. 2024 Jul 5;52(W1):W398–406.
54. Stadlbauer V, Horvath A, Komarova I, Schmerboeck B, Feldbacher N, Wurm S, et al. A single alcohol binge impacts on neutrophil function without changes in gut barrier function and gut microbiome composition in healthy volunteers. *PLOS ONE*. 2019 Feb 1;14(2):e0211703.
55. Lange EC, Rampelotto PH, Longo L, de Freitas LBR, Uribe-Cruz C, Alvares-da-Silva MR. Ornithine aspartate effects on bacterial composition and metabolic pathways in a rat model of steatotic liver disease. *World J Hepatol*. 2024 May 27;16(5):832–42.
56. Gerritsen J, Hornung B, Renckens B, van Hijum SAFT, Martins Dos Santos VAP, Rijkers GT, et al. Genomic and functional analysis of *Romboutsia ilealis* CRIBT reveals adaptation to the small intestine. *PeerJ*. 2017;5:e3698.
57. Efremova I, Alieva A, Maslennikov R, Poluektova E, Zharkova M, Kudryavtseva A, et al. *Akkermansia muciniphila* is associated with normal muscle mass and *Eggerthella* is related with sarcopenia in cirrhosis. *Front Nutr*. 2024;11:1438897.
58. Liwinski T, Hübener S, Henze L, Hübener P, Heinemann M, Tetzlaff M, et al. A prospective pilot study of a gluten-free diet for primary sclerosing cholangitis and associated colitis. *Aliment Pharmacol Ther*. 2023 Jan;57(2):224–36.
59. Wu Z, Pan D, Jiang M, Sang L, Chang B. Selenium-Enriched *Lactobacillus acidophilus* Ameliorates Dextran Sulfate Sodium-Induced Chronic Colitis in Mice by Regulating Inflammatory Cytokines and Intestinal Microbiota. *Front Med (Lausanne)*. 2021;8:716816.
60. Huang L, Yu Q, Peng H, Zhen Z. Alterations of gut microbiome and effects of probiotic therapy in patients with liver cirrhosis: A systematic review and meta-analysis. *Medicine (Baltimore)*. 2022 Dec 23;101(51):e32335.

61. Solé C, Guilly S, Da Silva K, Llopis M, Le-Chatelier E, Huelin P, et al. Alterations in Gut Microbiome in Cirrhosis as Assessed by Quantitative Metagenomics: Relationship With Acute-on-Chronic Liver Failure and Prognosis. *Gastroenterology*. 2021 Jan;160(1):206-218.e13.
62. Xu XT, Jiang MJ, Fu YL, Xie F, Li JJ, Meng QH. Gut microbiome composition in patients with liver cirrhosis with and without hepatic encephalopathy: A systematic review and meta-analysis. *World J Hepatol*. 2025 Jan 27;17(1):100377.
63. Bajaj JS, Thacker LR, Fagan A, White MB, Gavis EA, Hylemon PB, et al. Gut microbial RNA and DNA analysis predicts hospitalizations in cirrhosis. *JCI Insight*. 2018 Mar 8;3(5):e98019, 98019.
64. Llorente C, Jepsen P, Inamine T, Wang L, Bluemel S, Wang HJ, et al. Gastric acid suppression promotes alcoholic liver disease by inducing overgrowth of intestinal *Enterococcus*. *Nat Commun*. 2017 Oct 16;8(1):837.
65. Hanchi H, Mottawea W, Sebei K, Hammami R. The Genus *Enterococcus*: Between Probiotic Potential and Safety Concerns-An Update. *Front Microbiol*. 2018;9:1791.
66. Krawczyk B, Wityk P, Gałęcka M, Michalik M. The Many Faces of *Enterococcus* spp.- Commensal, Probiotic and Opportunistic Pathogen. *Microorganisms*. 2021 Sep 7;9(9):1900.
67. Rose C, Michalak A, Rao KV, Quack G, Kircheis G, Butterworth RF. L-ornithine-L-aspartate lowers plasma and cerebrospinal fluid ammonia and prevents brain edema in rats with acute liver failure. *Hepatology*. 1999 Sep;30(3):636-40.
68. Canbay A, Sowa JP. L-Ornithine L-Aspartate (LOLA) as a Novel Approach for Therapy of Non-alcoholic Fatty Liver Disease. *Drugs*. 2019 Feb;79(Suppl 1):39-44.
69. Aliwa B, Horvath A, Traub J, Feldbacher N, Habisch H, Fauler G, et al. Altered gut microbiome, bile acid composition and metabolome in sarcopenia in liver cirrhosis. *J Cachexia Sarcopenia Muscle*. 2023 Dec;14(6):2676-91.
70. Trieb M, Rainer F, Stadlbauer V, Douschan P, Horvath A, Binder L, et al. HDL-related biomarkers are robust predictors of survival in patients with chronic liver failure. *J Hepatol*. 2020 Jul;73(1):113-20.
71. Trieb M, Horvath A, Birner-Gruenberger R, Spindelboeck W, Stadlbauer V, Taschler U, et al. Liver disease alters high-density lipoprotein composition, metabolism and function. *Biochim Biophys Acta*. 2016 Jul;1861(7):630-8.
72. Ruan P, Gong ZJ, Zhang QR. Changes of plasma D(-)-lactate, diamine oxidase and endotoxin in patients with liver cirrhosis. *Hepatobiliary Pancreat Dis Int*. 2004 Feb;3(1):58-61.
73. Rainer F, Horvath A, Sandahl TD, Leber B, Schmerboeck B, Blesl A, et al. Soluble CD163 and soluble mannose receptor predict survival and decompensation in patients with liver cirrhosis, and correlate with gut permeability and bacterial translocation. *Aliment Pharmacol Ther*. 2018 Mar;47(5):657-64.
74. Blesl A, Jüngst C, Lammert F, Fauler G, Rainer F, Leber B, et al. Secondary Sclerosing Cholangitis in Critically Ill Patients Alters the Gut-Liver Axis: A Case Control Study. *Nutrients*. 2020 Sep 7;12(9):2728.
75. Li FC, Fan YC, Li YK, Wang K. Plasma diamine oxidase level predicts 6-month readmission for patients with hepatitis B virus-related decompensated cirrhosis. *Virology*. 2019 Sep 18;16(1):115.

76. Milbank E, Díaz-Trelles R, Dragano N, Latorre J, Mukthavaram R, Mayneris-Perxachs J, et al. Liver lipopolysaccharide binding protein prevents hepatic inflammation in physiological and pathological non-obesogenic conditions. *Pharmacol Res.* 2023 Jan;187:106562.
77. Agiasotelli D, Alexopoulou A, Vasilieva L, Hadziyannis E, Goukos D, Daikos GL, et al. High serum lipopolysaccharide binding protein is associated with increased mortality in patients with decompensated cirrhosis. *Liver Int.* 2017 Apr;37(4):576–82.
78. Wang D, Baghoomian A, Zhang Z, Cui Y, Whang EC, Li X, et al. Hepatic lipopolysaccharide binding protein partially uncouples inflammation from fibrosis in MAFLD. *J Clin Invest.* 2024 Sep 3;134(17):e179752.
79. Stasi A, Intini A, Divella C, Franzin R, Montemurno E, Grandaliano G, et al. Emerging role of Lipopolysaccharide binding protein in sepsis-induced acute kidney injury. *Nephrol Dial Transplant.* 2017 Jan 1;32(1):24–31.
80. Chen YY, Lien JM, Peng YS, Chen YC, Tian YC, Fang JT, et al. Lipopolysaccharide binding protein in cirrhotic patients with severe sepsis. *J Chin Med Assoc.* 2014 Feb;77(2):68–74.
81. Albillos A, de la Hera A, González M, Moya JL, Calleja JL, Monserrat J, et al. Increased lipopolysaccharide binding protein in cirrhotic patients with marked immune and hemodynamic derangement. *Hepatology.* 2003 Jan;37(1):208–17.
82. Jin CJ, Baumann A, Brandt A, Engstler AJ, Nier A, Hege M, et al. Aging-related liver degeneration is associated with increased bacterial endotoxin and lipopolysaccharide binding protein levels. *Am J Physiol Gastrointest Liver Physiol.* 2020 Apr 1;318(4):G736–47.
83. Eguchi A, Iwasa M, Tamai Y, Tempaku M, Takamatsu S, Miyoshi E, et al. Branched-chain amino acids protect the liver from cirrhotic injury via suppression of activation of lipopolysaccharide-binding protein, toll-like receptor 4, and signal transducer and activator of transcription 3, as well as *Enterococcus faecalis* translocation. *Nutrition.* 2021 Jun 1;86:111194.
84. Mookerjee RP, Stadlbauer V, Lidder S, Wright GAK, Hodges SJ, Davies NA, et al. Neutrophil dysfunction in alcoholic hepatitis superimposed on cirrhosis is reversible and predicts the outcome. *Hepatology.* 2007 Sep;46(3):831–40.
85. Tritto G, Bechlis Z, Stadlbauer V, Davies N, Francés R, Shah N, et al. Evidence of neutrophil functional defect despite inflammation in stable cirrhosis. *J Hepatol.* 2011 Sep;55(3):574–81.
86. Stadlbauer V, Mookerjee RP, Wright G a. K, Davies NA, Jürgens G, Hallström S, et al. Role of Toll-like receptors 2, 4, and 9 in mediating neutrophil dysfunction in alcoholic hepatitis. *Am J Physiol Gastrointest Liver Physiol.* 2009 Jan;296(1):G15-22.
87. Janani K, Jain M, Vargese J, Srinivasan V, Harika K, Michael T, et al. Health-related quality of life in liver cirrhosis patients using SF-36 and CLDQ questionnaires. *Clin Exp Hepatol.* 2018 Dec;4(4):232–9.
88. Les I, Doval E, Flavià M, Jacas C, Cárdenas G, Esteban R, et al. Quality of life in cirrhosis is related to potentially treatable factors. *Eur J Gastroenterol Hepatol.* 2010 Feb;22(2):221–7.
89. Bao ZJ, Qiu DK, Ma X, Fan ZP, Zhang GS, Huang YQ, et al. Assessment of health-related quality of life in Chinese patients with minimal hepatic encephalopathy. *World J Gastroenterol.* 2007 Jun 7;13(21):3003–8.

90. Fabrellas N, Moreira R, Carol M, Cervera M, de Prada G, Perez M, et al. Psychological Burden of Hepatic Encephalopathy on Patients and Caregivers. *Clin Transl Gastroenterol*. 2020 Apr;11(4):e00159.
91. Nagel M, Weidner V, Schulz S, Marquardt JU, Galle PR, Schattenberg JM, et al. Continued alcohol consumption and hepatic encephalopathy determine quality of life and psychosocial burden of caregivers in patients with liver cirrhosis. *Health Qual Life Outcomes*. 2022 Feb 8;20(1):23.
92. Montagnese S, Amato E, Schiff S, Facchini S, Angeli P, Gatta A, et al. A patients' and caregivers' perspective on hepatic encephalopathy. *Metab Brain Dis*. 2012 Dec;27(4):567–72.
93. Ong JP, Oehler G, Krüger-Jansen C, Lambert-Baumann J, Younossi ZM. Oral L-ornithine-L-aspartate improves health-related quality of life in cirrhotic patients with hepatic encephalopathy: an open-label, prospective, multicentre observational study. *Clin Drug Investig*. 2011;31(4):213–20.
94. Pasha Y, Taylor-Robinson S, Leech R, Ribeiro I, Cook N, Crossey M, et al. PWE-091 L-ornithine L-aspartate in minimal hepatic encephalopathy: possible effects on the brain-muscle axis? *Gut*. 2018 Jun 1;67(Suppl 1):A117–8.
95. Kircheis G, Nilius R, Held C, Berndt H, Buchner M, Görtelmeyer R, et al. Therapeutic efficacy of L-ornithine-L-aspartate infusions in patients with cirrhosis and hepatic encephalopathy: results of a placebo-controlled, double-blind study. *Hepatology*. 1997 Jun;25(6):1351–60.
96. Stauch S, Kircheis G, Adler G, Beckh K, Ditschuneit H, Görtelmeyer R, et al. Oral L-ornithine-L-aspartate therapy of chronic hepatic encephalopathy: results of a placebo-controlled double-blind study. *J Hepatol*. 1998 May;28(5):856–64.
97. Butterworth RF, McPhail MJW. L-Ornithine L-Aspartate (LOLA) for Hepatic Encephalopathy in Cirrhosis: Results of Randomized Controlled Trials and Meta-Analyses. *Drugs*. 2019 Feb;79(Suppl 1):31–7.
98. Jhajharia A, Singh S, Jana S, Ashdhir P, Nijhawan S. Intravenous versus oral 'L-ornithine-L-aspartate' in overt hepatic encephalopathy: a randomized comparative study. *Sci Rep*. 2024 May 24;14(1):11862.
99. Davenport A, Cholongitas E, Xirouchakis E, Burroughs AK. Pitfalls in assessing renal function in patients with cirrhosis--potential inequity for access to treatment of hepatorenal failure and liver transplantation. *Nephrol Dial Transplant*. 2011 Sep;26(9):2735–42.
100. Butterworth RF. L-Ornithine L-Aspartate for the Treatment of Sarcopenia in Chronic Liver Disease: The Taming of a Vicious Cycle. *Can J Gastroenterol Hepatol*. 2019;2019:8182195.
101. Kumar A, Davuluri G, Silva RNE, Engelen MPKJ, Ten Have GAM, Prayson R, et al. Ammonia lowering reverses sarcopenia of cirrhosis by restoring skeletal muscle proteostasis. *Hepatology*. 2017 Jun;65(6):2045–58.